

TENSILE LAP SPLICES

PART 2: DESIGN RECOMMENDATIONS FOR RETAINING WALL
SPLICES AND LARGE BAR SPLICES

by

Phil M. Ferguson

and

C. N. Krishnaswamy

Research Report No. 113-3

Research Project Number 3-5-68-113
Splices and Anchorage of Reinforcing Bars

Conducted for

The Texas Highway Department

In Cooperation with the
U. S. Department of Transportation
Federal Highway Administration

by

CENTER FOR HIGHWAY RESEARCH
THE UNIVERSITY OF TEXAS AT AUSTIN

April 1971

P R E F A C E

This Part 2 (Research Report 113-3) is a final report on all those phases of the general project "Splices and Anchorage of Reinforcing Bars" which relate to tensile bar splicing. It follows Research Report 113-2 "Tensile Lap Splices, Part 1: Retaining Wall Type, Varying Moment Zone," and reports further tests with #11, #14, and #18 reinforcing bars. All the splice tests are analyzed as a group and conclusions and recommendations are made which are more inclusive and general than those made in Part 1. Part 1 should now be considered as superseded by this Part 2.

In the Preface to Part 1, two separate follow-up reports, Part 2 and Part 3, were mentioned. These have been combined into the present single report.

Research Report 113-1, entitled "Test of Upper Anchorage No. 14S Column Bars in Pylon Design," by K. S. Rajagopalan and Phil M. Ferguson, published August 1968, covers another separate phase of the project completed earlier. Later reports will cover some bracket-shear problems and a look at the influences of bond creep on deflections.

Support has been provided by the Texas Highway Department and the U. S. Department of Transportation Federal Highway Administration. The encouragement and assistance of the contact representatives are acknowledged with thanks.

The opinions, findings, and conclusions expressed in this publication are those of the authors and not necessarily those of the Federal Highway Administration.

C. N. Krishnaswamy
Phil M. Ferguson

March 1971

A B S T R A C T

As a continuation of Report 113-2 an additional 32 full size beams were tested with #5 (1 beam), #11, #14, and #18 tension bar splices. The needed splice length is subject to the obvious variables, including bar stress f_s , concrete strength f'_c , bar diameter D , clear lateral spacing S' , and to a new coefficient (less than unity) which is largely defined by the ratio S'/C , the ratio of the net width of concrete between bars (typically the clear splice spacing S') to the clear cover C . In a smaller way this coefficient is also a function of f_s . The ratio of S'/C determines the type of splice failure to be expected.

Recommended design equations are presented, which include a reserve to develop toughness in the member. In general, the 1969 AASHTO specification is shown to be inadequate except for small bar sizes and large lateral spacings of splices.

Retaining wall splices, except for the end splice in the wall, are safe with a lap about 15 percent shorter and may be further shortened to recognize the average bar stress at the two ends of the splice rather than the higher stress at the base.

Splices for Grade 40 bars may be made only 57 percent of the length required for Grade 60 bars. For top-cast bars, splices in lightweight concrete, etc., the usual special factors apply.

Tentative requirements for ties or spirals over the splices are presented in terms of the added splice stress f_{st} which should be developed in the splice.

Lap splices for #14 or #18 bars may be designed under the same rules as smaller bars insofar as strength is concerned, but the use of transverse ties with large bar splices is recommended. The widths of cracks increase as bar size increases, such that the cracks at the end of a lap splice for a #18 bar could be of concern in some exposures. (Even with an unspliced bar there is more cracking with a #18 bar than with smaller sizes.)

The Cadweld splicing of #18 bars, on a sampling basis, proved satisfactory in developing flexural failures, with about the same crack problem as with the lap splices.

The design requirements presented for lap splices are the most advanced and best documented to date. Those for splices without ties or spirals are ready for inclusion in design codes.

The use of some ties (or a spiral) over lap splices adds to toughness and should be required on #18 bar splices. Further study of their effectiveness in terms of possible reduced lap is desirable.

S U M M A R Y

As a continuation of Report 113-2 an additional 32 full size beams were tested with large bar splices.

In addition to the usual variables, the ratio S'/C , the clear spacing between splices to clear cover over them, was found to be an important variable. This ratio determines the type of splice failure to guard against.

Recommended design equations are presented. In general, the AASHO specification is shown to be inadequate except for small bar sizes and large lateral spacings of splices. The lap required for Grade 60 bars fully stressed in 3000 psi concrete is

$$\text{Design } L_{s60} = 100D^2 \left(\frac{1}{S'} + \frac{1}{2C} \right) \geq 100D^2 (1.5/S')$$

with the usual modifications for top-cast bars, lightweight concrete, etc. This equation shows clear cover C to be equally as important as clear spacing S' , considering the fact that cover C is usually numerically smaller than the spacing S' .

For Grade 40 steel the splice length can be 0.57 of the Grade 60 length, the length dropping more than the yield stress.

Splices in retaining walls, except for the end splice at each expansion joint, can be reduced by substituting (in the L_{s60} equation) $42(1+k)$ in place of 100, with k the ratio of the steel stress at the top of the splice to that at the base, a factor always less than unity.

Tentative requirements for ties or spirals over the splices are presented in terms of the added splice stress f_{st} which should be developed in the splice.

Lap splices for #14 or #18 bars may be designed under the same rules as smaller bars insofar as strength is concerned. The use of transverse ties with large bar splices is recommended. The widths of cracks increase as bar size increases, such that the cracks at the end of a lap splice for a #18 bar could be of concern in some exposures. (Even with an unspliced bar there is more cracking with a #18 bar than with smaller sizes.)

The Cadweld splicing of #18 bars, on a sampling basis, proved satisfactory in developing flexural failures, with about the same crack problem as with the lap splices.

The design requirements presented for lap splices are the most advanced and best documented to date. Those for splices without ties or spirals are ready for inclusion in design codes.

The use of some ties (or a spiral) over lap splices adds to toughness and should be required on #18 bar splices. Further study of their effectiveness in terms of possible reduced lap is desirable.

I M P L E M E N T A T I O N

The design recommendations contained in this report in terms of the required lengths of tension lap splices are sufficiently established to be incorporated at once into structural design specifications. For the first time they reflect the effect of clear cover over the bars and they refine the requirements for varying clear spacing more consistently than any previous formulations.

Splices based on the 1969 AASHTO specifications are inadequate except for small bar sizes and for very large lateral spacings of larger bar splices. Safety requires the rewriting of this specification to the level indicated in the Conclusions to Part A (pages 17 and 18). Wall splices and the evaluation of transverse reinforcement are less urgent matters.

Retaining wall splices, except for the end splice in the wall, can be shorter than in beams by at least 16 percent and by a somewhat larger percentage when the stress at the top of the splice is included in the calculations.

Lap splices with #14 bars, especially if with transverse ties, should no longer be prohibited. Possibly similar splices of #18 bars should be permitted; they are satisfactory for strength but involve wider flexural cracks.

Splice behavior with ties over the splices is so much improved that a specification requiring ties should be considered. In such a case, the tentative recommendations as to the strength accruing should be further studied experimentally to firm up the recommendations and establish minimum quantities to be used.

I N T R O D U C T I O N

Existing Splice Requirements

Some of the inadequacies of splice design of reinforcing bars under the 1965 AASHTO Specifications and the 1963 ACI Building Code were pointed out in Report 113-2 (July 1969) which constituted Part 1 of this project.

The 1969 AASHTO Specification states splices shall not be at points of maximum stress, but permits laps on Grades 40 and 50 which, if extrapolated to Grade 60, lead to the following lap splice lengths L_s for a bar diameter D in 3000 psi or higher strength concrete:

24D for Grade 40

30D for Grade 50

36D for Grade 60

The ACI Building Code (318-63) for splices spaced closer than 12D requires 20 percent more lap than $L_s = f_y D / 4u$, where u is 3/4 of the generally allowable $u = 9.5 \sqrt{f'_c} / D$:

$$L_s = f_y D^2 / (23.7 \sqrt{f'_c}) = 0.00077 f_y D^2 \text{ for } f'_c = 3000 \text{ psi}$$

For f_y of 40,000 psi, $L_s = 28.5D^2$ or 40.2D for #11 bars

For f_y of 60,000 psi, $L_s = 42.7D^2$ or 60.3D for #11 bars

Both regulations call for longer laps for top* bars and forbid lap splices of #14 and #18 bars.

The Part 1 report recommended for retaining wall splices with 2 in. of clear cover, f_y of 40,000 psi, and f'_c of 3500 psi, a length based on S/D , the ratio of center-to-center spacing S to bar diameter D :

$$L_s = 19D \div (0.13 S/D - 0.04) \geq 19D.$$

The present report defines the needs better, and in some cases more restrictively, by recommendations based on clear spacing S' between splices and clear cover C .

*Top bars are bars having more than 12 in. of concrete cast in the member below the bar.

Project Objectives

This project has studied general lap splice behavior in order to answer several specific questions.

- (1) How does splice strength vary with spacing and cover, in beams and in walls?
- (2) Can #14 and #18 bars be lap-spliced?
- (3) How effective are ties or spirals around a lap splice?
- (4) Is the behavior of a #18 bar Cadweld splice in a beam satisfactory?

An effort has been made to build the answers to the first and second questions into a more general procedure for analysis or design of tension splices.

Scope of Investigation

Thirty-two splice (beam) specimens were designed and tested in addition to the 32 reported earlier (Report 113-2). An additional 53 specimens from other investigations were studied and used in the analysis reported. Only deformed bars were considered.

Of the 32 new specimens, 11 contained #11 bar splices, 1 - #5 bar splices, 7 - #14 bar splices, and 15 - #18 bar splices. Of the #18 bar splice beams, 3 contained Cadweld splices instead of lapped bars.

Organization of Report

The report which follows is presented in three sections:

Part A gives a summary type of report consisting of an overall view of the analysis with emphasis on adaptations and conclusions of interest to the designer.

Part B covers the specimen descriptions, the tests, and data analysis in more detail.

The Appendix includes pertinent data tables, and a table of notation.

P A R T A - A N A L Y S I S S U M M A R Y

LAP SPLICES WITHOUT TRANSVERSE REINFORCEMENT

Variables

The two most important variables defining splice strength, other than splice length, the material strengths, and the bar diameter, proved to be the clear lateral spacing S' (net concrete width) between adjacent splices and the clear cover C over the splices.

Since splice strength was found not to vary entirely linearly with either length or lateral spacing of adjacent splices, the analysis presented earlier (Report 113-2) was found more useful as a general guide than as a design tool. The general picture of splice failure as a splitting failure and the several types of failure patterns in that report remain intact.

Damage resulting at ultimate from large concrete strains at the continuing end of the lapped bar reduced the observed resistance in that region while near the free end of the bar tensile stress was built up rapidly. Laterally the average tensile stress in the concrete appeared to be more nonuniform as the spacing between adjacent splices was increased. The analysis selected as most suitable involves a ratio α between (a) the average splitting stress and (b) the split cylinder tensile strength of the concrete, taken here as $6.4\sqrt{f'_c}$. The splitting stress, over the entire splice length L_s and the entire net concrete width S' per splice, is calculated to resist an assumed splitting force related to the bond stress.

Basic Strength Equation

The lateral splitting forces from each bar were assumed to have a radial unit intensity (like water pressure in a pipe) equal to the average bond stress on the bar, as sketched in Fig. 1. The total pressure on the horizontal plane from two identical bars making up one splice over the splice length becomes

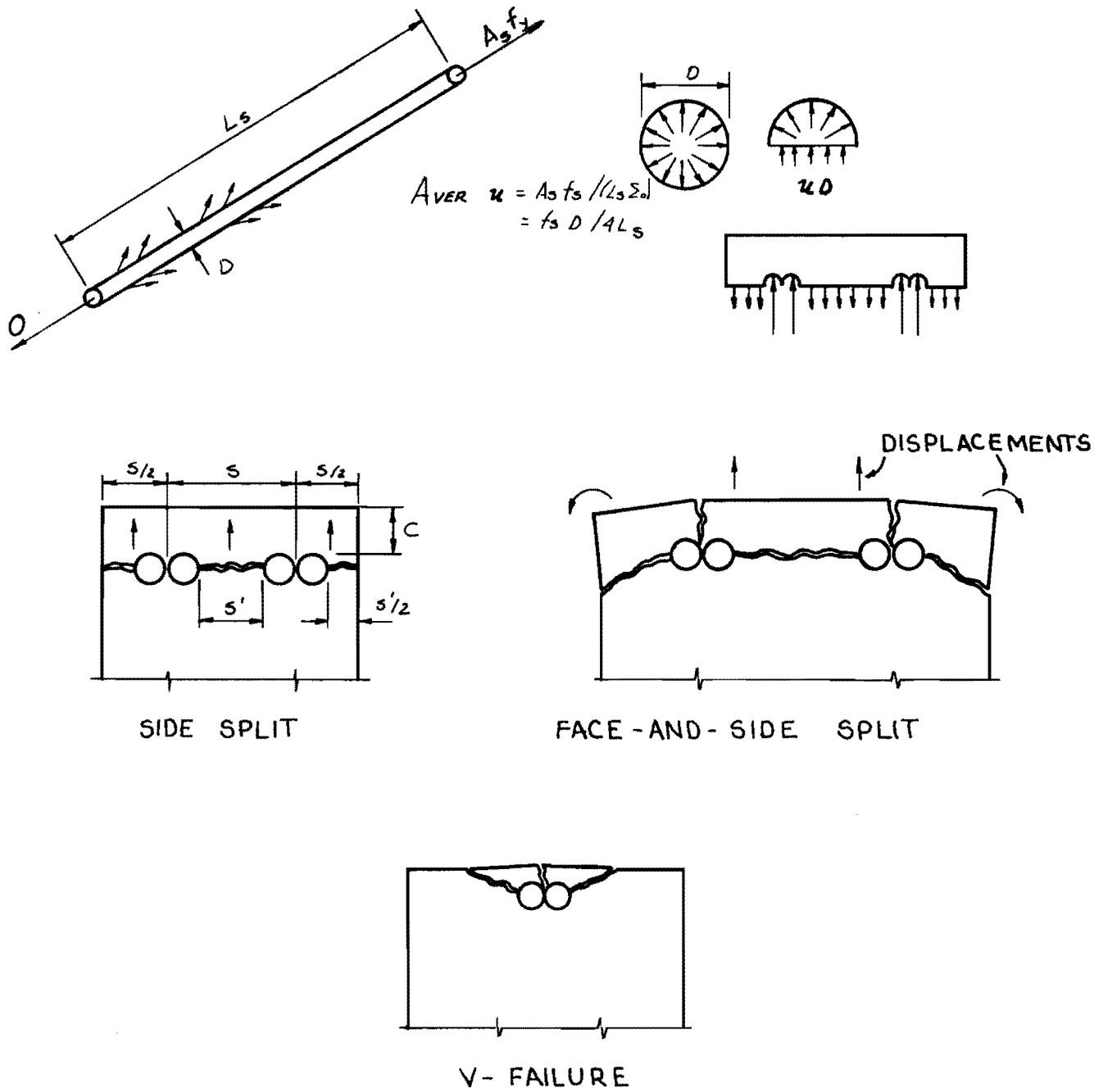


Fig. 1. Splitting around splices.

$$2D(f_s D/4L_s)L_s = f_s D^2/2$$

which must be resisted by an average tensile stress $\alpha(6.4\sqrt{f'_c})$ over a concrete area $S'L_s$. As used, α reflects not only nonuniform stress resistance lengthwise and transversely but also possible variations in the developed radial pressure resulting from varying confinement or cover. From the equality of force and resistance at ultimate the required L_s is

$$L_s = \frac{f_s D^2/2}{\alpha 6.4\sqrt{f'_c} S'} = 0.0782f_s D^2/(\alpha\sqrt{f'_c} S') \quad (1)$$

The above analysis indicates that S' is a more logical variable than S . In reconsideration of the previous report, it also became evident that the clear cover C would be important in determining the break points between the three types of failure observed and shown in Fig. 1:

Close S'/C	Side split, across the plane of the bars
Intermediate S'/C	Face-and-side split, as in side split except that splits to the tension face trigger failure
Very wide S'/C	V-type, creating a V-shaped trench over the splice, with concrete pushed out after longitudinal splitting forms on the tension face

When all pertinent data were plotted* in terms of α against S'/C in Fig. 2, these break points were evident (charted at the bottom of the figure) and a lower bound curve could be sketched by excluding only splices at very high stresses. The α values of this lower bound curve were then replotted as $1/\alpha$ in Fig. 3 and formed essentially a straight line. This upper bound line has the equation

$$1/\alpha = 0.9 + 0.45 S'/C = 0.9(1 + 0.5 S'/C) \quad (2)$$

which is appropriate as an analysis equation for f_s at least up to 60,000 psi.

*Data from Appendix Tables A.1 through A.3. The number by each point denotes splice length in bar diameters, a y indicates yield of the bars, and three cases with $f_s > 80$ ksi are noted with the stress itself.

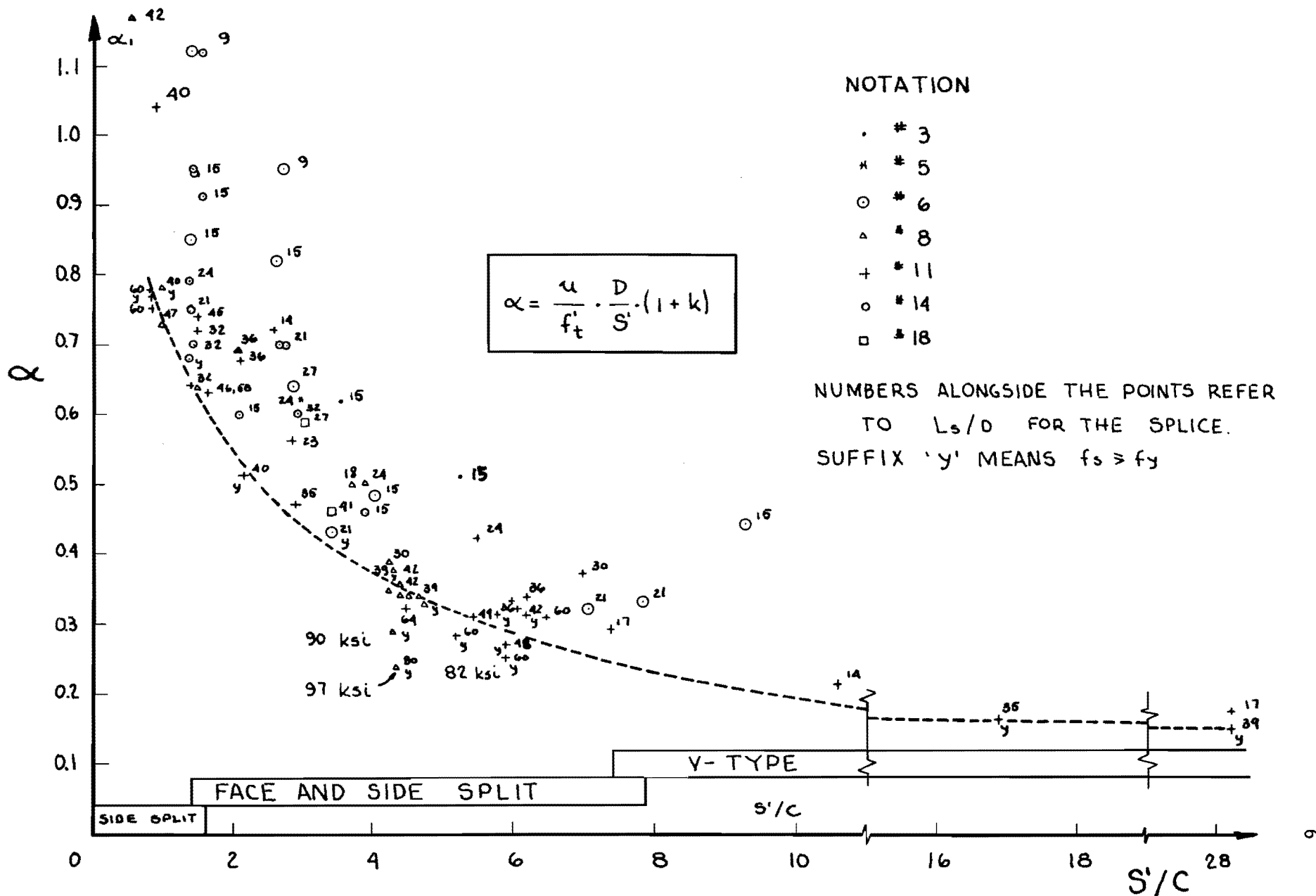


Fig. 2. Variation of α with S'/C .

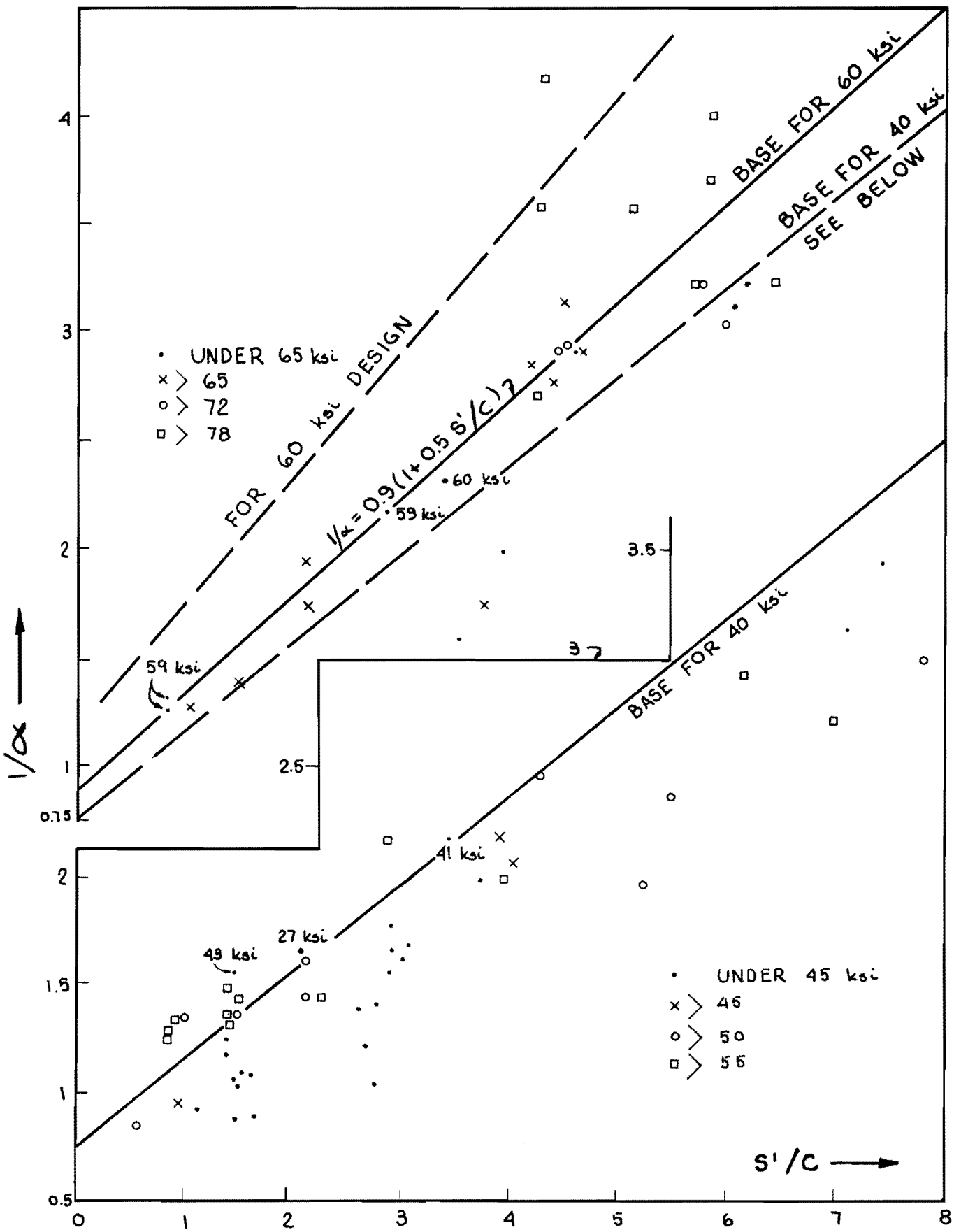


Fig. 3. Variation of $1/\alpha$ with S'/C and safe bounds.

When f_s of 60,000 psi, f'_c of 3000 psi, and $1/\alpha$ from Eq. 2 are inserted into Eq. 1, the theoretical required splice length, without including necessary modification to maintain ductile behavior, becomes

$$L_s = 77D^2(1 + 0.5 S'/C)/S' \doteq 77D^2\left(\frac{1}{S'} + \frac{1}{2C}\right)$$

Design Equation for Grade 60 Bars

For Grade 60 reinforcement a sudden brittle failure at 60 ksi is not acceptable. A design for a stress of 75 ksi (25 percent extra)* would be in the direction of ductility and would call for a factor of $75/60 = 1.25$ for stress alone and some additional amount for a lowered α , say, a factor of 1.30 overall, which leads to

$$\text{Design } L_{s60} = 100D^2\left(\frac{1}{S'} + \frac{1}{2C}\right) \quad (3)$$

When C is greater than S' , it is recommended that the parenthesis in this and all later design equations be taken $1.5/S'$, equivalent to substituting S' for C . There are inadequate data to say now whether a greater C would be effective in this range. This applies in 3000 psi concrete to all sizes of Grade 60 bars in a constant moment region, but requires modification for "top" bars or lightweight concrete.

Staggered Splices

For staggered splices not involving a splice close to a corner, the same equation is usable if S' is taken as the total available width of resisting concrete, i.e., the doubled center-to-center spacing less $3D$. If splice stagger is applied to the case of only two bars symmetrically placed in a beam, the effective S' may be nearer 1.5 times the value for all bars spliced. Likewise, if a single splice is near a beam corner, the effective S' should not be taken more than about 3 times the edge cover over the bar.

Splices in a Variable Moment Region

For retaining wall splices of one bar size at the base of the stem, the main stem bars will have a lower stress kf_y at the top of the splice,

*Or possibly a unit steel strain of 0.01 in./in. if it occurs at a stress less than 75 ksi would be as effective.

where $k < 1$. The average bar stress governs the splice length, that is, Eq. 3 may be multiplied by the ratio $(1 + k)/2$, provided $k \geq 0.5$.

$$\text{Design } L_{s60} = 50(1 + k)D^2 \left(\frac{1}{S'} + \frac{1}{2C} \right) \quad (3a)$$

If k is 0.5, L_s reduces to 75 percent of the Eq. 3 value. There are no data for $k < 0.5$ and at $k = 0$ the concept leads to false values of development length.

Interior Splices in Walls and Slabs

In a beam a face-and-side split failure occurs when $S'/C > 1.7$ or 1.8, as indicated at the bottom of Fig. 2. Such a splice is weak, because the corner element (eccentrically loaded after the face crack, as in Fig. 21 of Part B) is weak and this lowers the possible α , as already reflected in Eq. 3. If in a continuous wall the extreme end bar splices in the wall are designed to this standard (and preferably staggered), the other (interior) splices appear to avoid this complication; they need not be controlled by a corner element.

Two attempts were made to evaluate this favorable wall condition numerically with beams carrying three splices spaced at S' more than $1.8C$. (The effect of 4 closely spaced splices had earlier resulted in a side split failure.) At a wider spacing, if the corner splices retained the average spacing, no extra advantage accrued because of the extra (third) middle splice. With an increased distance from corner to outside splices, corner failure was avoided; but it was then impossible to allocate the extra strength obtained between the partial V-type failure at the outside splices and the improved interior splice. Rated on the basis of the center spacing alone, the gain in strength for the entire group was 40 percent; but the adjacent half V-type failures undoubtedly contributed part of this gain.

Interior Wall Splice Recommendation

Wall splices deserve further study with very wide wall type sections containing special corner splices (probably also staggered) and some 4 to 6 interior splices. Pending such experimental proofs, the authors recommend, on the basis of judgment and the one test above, an allowance of 20 percent more strength on interior wall splices having $S'/C \geq 2$, that is, a required

L_s taken as 0.83 of Eq. 3 lengths. This factor would be superimposed on the usual correction for lower stress at one end of the splice.

$$\begin{aligned} L_{s60w} \text{ for interior wall splice} &= 0.83\left(\frac{1+k}{2}\right)100D^2\left(\frac{1}{S'} + \frac{1}{2C}\right) \\ &= 42(1+k)D^2\left(\frac{1}{S'} + \frac{1}{2C}\right) \quad (4) \end{aligned}$$

This equation appears valid for Grade 60 steel in any wall or slab situation which avoids the weak corner element concept, provided $S' \geq 2C$.

Design Equation for Grade 40 Bars

One of the factors causing scatter in the test values plotted in Fig. 2 is that of splice length. Each of the plotted points has alongside it a number indicating the splice length in bar diameters. The points generally arrange themselves with short lengths at the top of the scatter and longer lengths nearer the lower bound curve. The shorter lengths result in a better distribution of splitting resistance. If one uses Grade 40 bars, Eq. 1 indicates the use of a lower L_s because of the lower f_y and Fig. 2 suggests the lower L_s probably justifies a higher α . A study of this relation suggests that for $S'/C \geq 2$ the value of $1/\alpha$ may safely be taken as 0.85 of the value in Eq. 2. With the 40/60 factor for f_y and the 0.85 factor for $1/\alpha$ multiplied into Eq. 3

$$\text{Design } L_{s40} = 57D^2\left(\frac{1}{S'} + \frac{1}{2C}\right) \geq 57D^2(2/S'). \quad (5)$$

This again is based on 3000 psi concrete and requires modification if used for top bars as defined in the AASHTO and ACI documents. For interior wall splices with Grade 40 bars the lengths of Eq. 4 may also be multiplied by the same 0.57 factor where $S'/C \geq 2$. For $S'/C < 2$, replace $1/2C$ by $1/S'$.

Concrete Strengths Other Than 3000 psi

For f'_c values other than 3000 psi, the required L_s in Eqs. 3, 4, and 5 should be multiplied by $\sqrt{3000/f'_c}$. There is no need under these relations to set an upper limit of 3500 psi to the f'_c used (as the 1969 AASHTO Specification does).

V-Type Failures--The Optimum in Splice Strength

When splice spacing is very wide, $S'/C \geq 7.5$ or 8, the V-type failure of each splice mobilizes all the available concrete resistance around it and splice strength is independent of the neighboring splices. In this rather uncommon range the α versus S'/C relation (Fig. 2) is a curve only because some useless width has been included in S' ; the splice strength itself is constant and cannot be strengthened by more width. Although data here are limited, acceptance of the lower bound curve of Fig. 2 provides data for an estimate of the necessary L_s from Eq. 3 or Eq. 5. In a constant moment region at $S'/C = 8$ or $S' = 8C$, the equations become (for $f'_c = 3000$ psi)

$$\text{Design } L_{s60v} = 100D^2 \left(\frac{1}{8C} + \frac{1}{2C} \right) = 63D^2/C \quad (6a)$$

$$\text{Design } L_{s40v} = 57D^2 \left(\frac{1}{8C} + \frac{1}{2C} \right) = 36D^2/C \quad (6b)$$

These lengths, for Grades 60 and 40, respectively, may be considered minimum acceptable L_s values in a constant moment region for fully developed isolated splices where only a V-type failure is possible. However, in a nonuniform moment region the $(1+k)/2$ reducing factor is always valid and may be used in Eq. 6a or 6b. Most splices are closer spaced, except possibly in walls, and require greater lengths.

Because a V-type failure and a side split wall failure represent different S'/C values, Eq. 4 for walls cannot be used in this connection except to establish the particular S'/C which gives equal strengths and required L_s values. Equating Eq. 4 (with $k = 1$) to Eq. 6a

$$84D^2 \left(\frac{1}{S'} + \frac{1}{2C} \right) = 63D^2/C$$

leads to a value of $S'/C = 4$. Since Eq. 4 includes a judgment factor, the result is very approximate and possibly the conclusion should be that the breakpoint is around 4 or 5. Larger S'/C values in walls should lead to the V-type failure.

Comparisons with AASHO and ACI Specifications

Comparisons are clearer in graphical form, because of the number of variables as well as the two reference standards (AASHO and ACI) and the earlier Report 113-2. For beams the large influence of the clear spacing is indicated in Fig. 4a, c, along with the fact that the AASHO Specification is always on the unsafe side at $S' = 4$ in. for all bars larger than #6. The 1963 ACI Code is not far from what is needed at a clear spacing of 4 in., but is far deficient at a closer spacing, such as $S' = 2$ in.

For walls, Fig. 4b, c, the major emphasis of this investigation, recognition that splice design can be based on the average stress at the two ends of the splice can lead to a worthwhile saving, as indicated by the range in the hatched areas between $k = 1.0$ and $k = 0.6$, where k is the ratio of the smaller stress to the larger. A k of 0.6 can mean a saving of 20 percent on the required lap. The present investigation has lowered the recommended L_s noticeably from that in Report 113-2, except for large bars at 60 ksi. Further study of the wall situation is justified since the current recommendation involved a judgment which may well have been over-conservative.

TENSILE SPLICES OF #14 AND #18 BARS

Present Design Status

Both the AASHO and ACI standards permit no tensile lap splicing of bars larger than #11. Welded splices or other positive connections must be used for #14 and #18 bars and must develop 125 percent of the bar yield strength.

Overall Experimental Conclusions

Without transverse reinforcement #14 and #18 bars can be lap spliced in tension to a capacity adequate for Grade 40 bars by using Eq. 5. It may be possible to splice higher strength bars in this manner, but (1) the splices would be very long, and (2) the slow rate of increase in strength with added length leaves some uncertainty about the chances. For example, in the only available comparison with #18 bars, a 55 percent

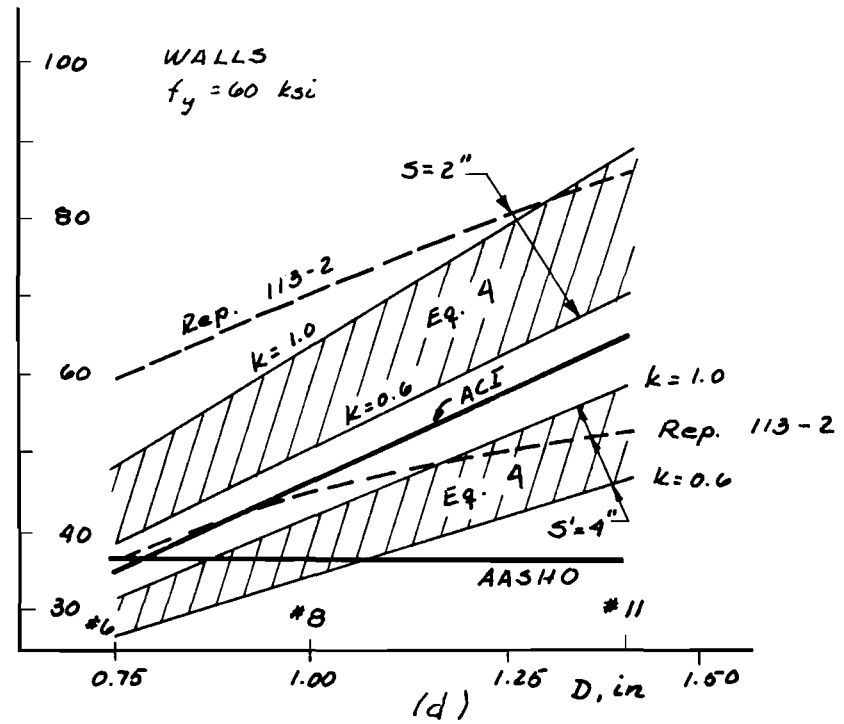
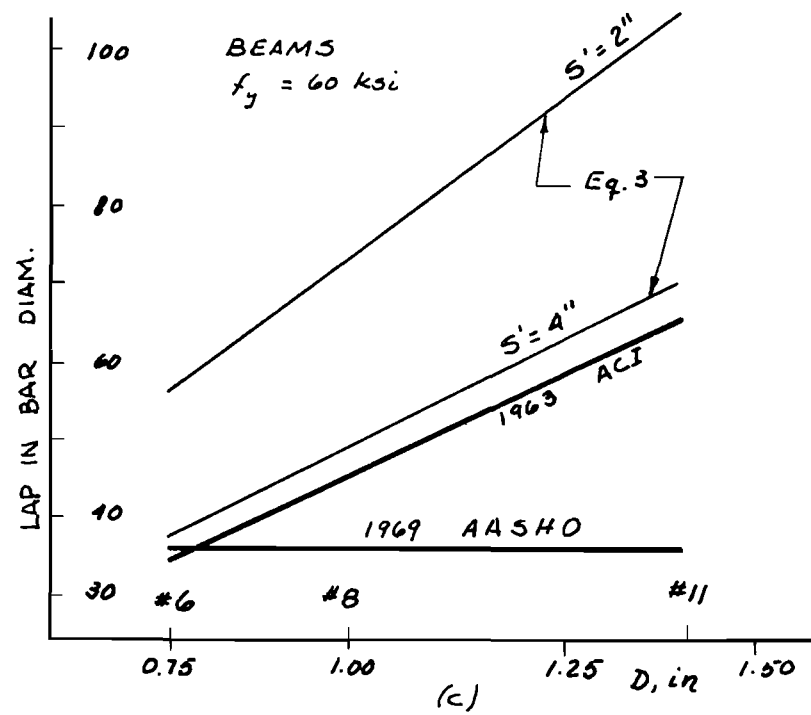
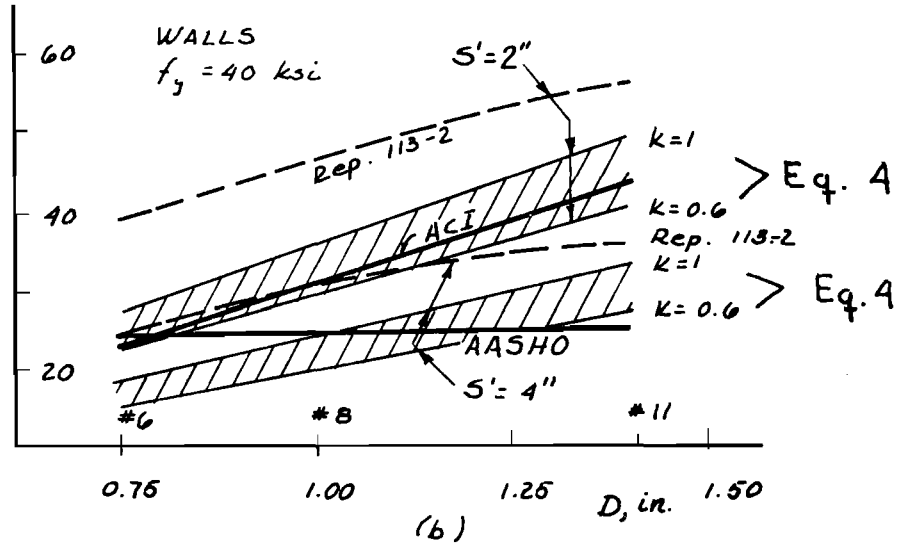
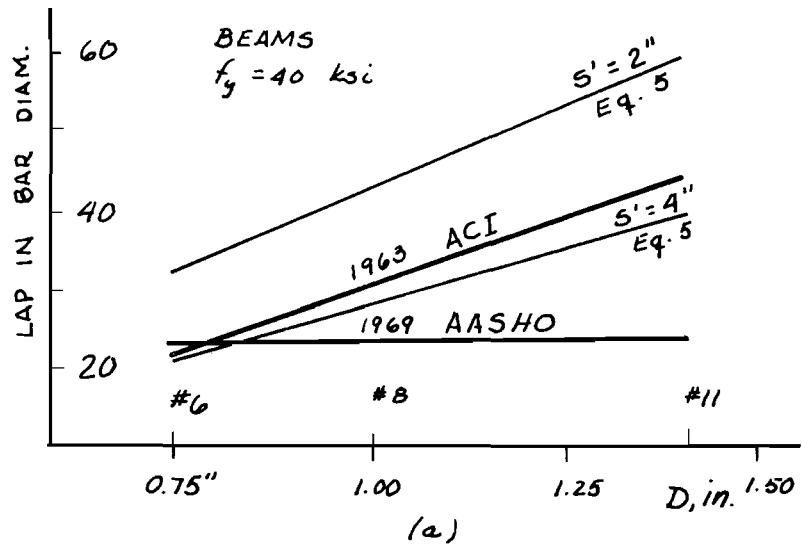


Fig. 4. Recommended lap splice lengths, $C = 2''$, $f'_c = 3000$ psi.

increase (33 in.) in L_s in a concrete 90 percent as strong and providing 88 percent the clear cover increased the maximum steel stress only from 45.2 ksi to 51.5 ksi (14 percent).

With transverse reinforcement, either ties or spirals, no problem exists in developing both strength and ductile behavior with Grade 60 bars. Designs with transverse reinforcement lead to a more ductile failure and also are probably more economical. The limited data available show maximum crack widths at the ends of splices a little less severe with spirals than with stirrups. The design method for transverse reinforcement is covered in the next major section. In the absence of other sources, lap splice design for the #14 and #18 bars appears feasible simply on the basis of the design equations for smaller bars, preferably with the use of transverse reinforcement as specified in the next major section.

Crack Widths

At the point where the bars are cut off extra crack widths occur, the increase over normal being some function of the percentage of bars cut off. In 1965, Ferguson and Breen reported,¹ at a service load stress of 36 ksi, average end crack widths of 0.0094 in. for #8 splices and 0.0097 in. for #11 splices without stirrups. In each case the clear cover was 1.5 in., which is important because crack width varies almost linearly with clear cover.

For #14 splices with 2.4 in. clear cover over the bars (not over the stirrups or spirals), the corresponding maximum (end) crack width (Fig. 5a) on a specimen with spirals was 0.0130 in., and with stirrups 0.0150 in., these being reduced by at least 12 percent when both ends were averaged (Fig. 5b). If allowance is made for the difference in cover, a ratio of 2.4/1.5, these data compare very closely with the #11 bar data above and are better than the 0.016 in. reported in the case of #11 bars with stirrups.

For #18 splices with 3 in. clear cover over the bars (not over the spirals) the corresponding maximum crack width on a specimen with spirals was 0.0195 in. and without transverse reinforcement 0.0245 in., with the averages at the two ends 0.018 and 0.016 in., respectively. For appearance, the #18 splice cracks are obviously worse with the 3 in. cover. Whether the basic crack width at the bar is significantly wider and whether this cracking increases the chance of corrosion is not clear from the data,

¹Ferguson, Phil M., and Breen, John E., "Lapped Splices for High Strength Reinforcing Bars," Journal of the American Concrete Institute, Proc. V. 62 (September 1965), pp. 1063-1078.

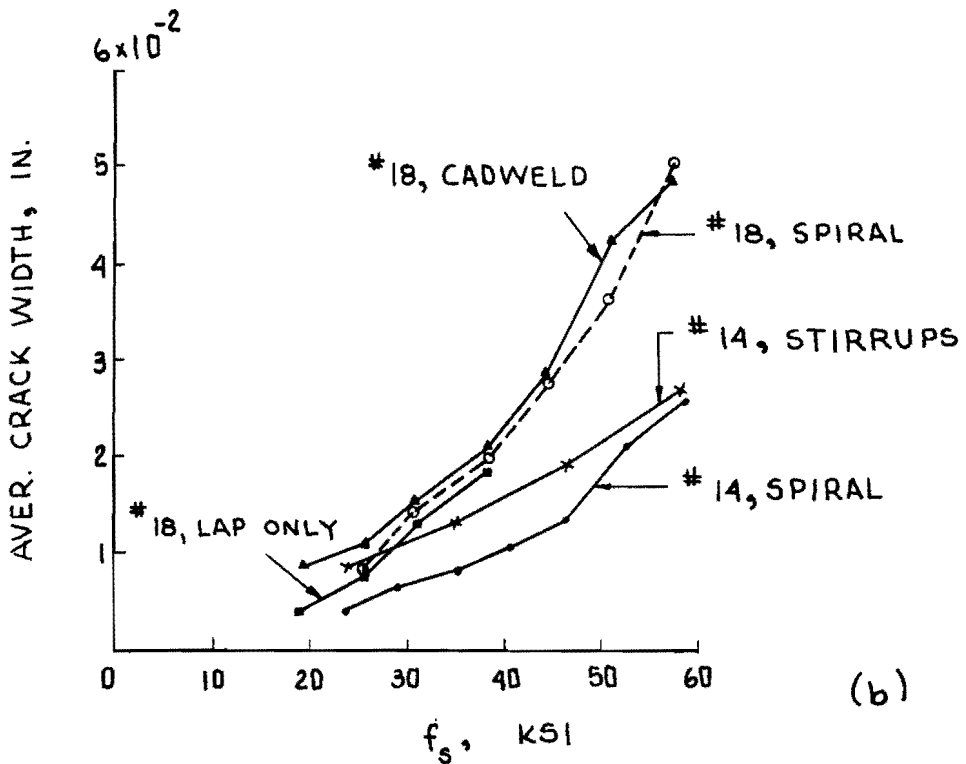
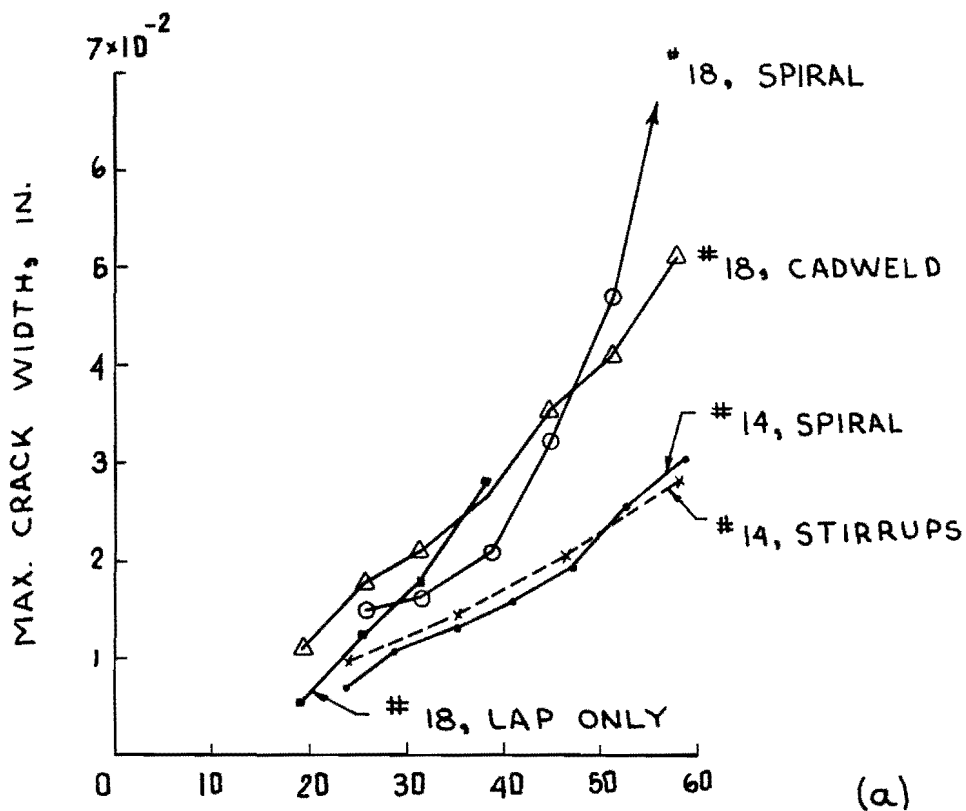


Fig. 5. Flexural crack widths at splice ends, #14, #18.
 (a) Maximum observed.
 (b) Average end cracks.

since $(1.5/3.0)0.018 = 0.009$ in., about the same as for the #8 splices.

In a particularly corrosive atmosphere or exposure to chlorides (salt water), there is some question raised by these crack sizes at #18 bar splices. Grade 40 bars at service load stresses of 24 ksi, however, present no more problems than are normally present for #11 bars. It is noted that the Cadweld splice with the #18 bars presented the same crack problem and it almost surely exists wherever a tension bar of this area is cut off and terminated in other than a compression region.

DESIGN OF TRANSVERSE REINFORCEMENT

In part B it has been found expedient to express the total strength of a splice as the sum of its strength based on the concrete without transverse reinforcement plus the added strength because of the spirals or ties.* For a given f_{st} to be added to the splice capacity the equation developed is:

$$\begin{aligned} \text{Reqd. } A_v f_{yt} &= 0.13(1 + k)f_{st} D^2 (1 + 2S'/C) \\ &= 0.26 f_{st} D^2 (1 + 2S'/C) \text{ for } k = 1 \end{aligned} \quad (7)$$

where A_v represents the total area of all transverse steel (both stirrup legs if the stirrup is not shared with other splices) with a yield strength f_{yt} . The second form of the equation applies in a constant moment zone. Equation 7 is not as solidly established as the earlier design equations presented, but seems adequate with almost all test data (3 exceptions noted in Fig. 24). No differentiation is yet made between spirals and ties, although spirals appear to perform a little better overall.

CADWELD SPLICE EFFECTIVENESS

Questions have occasionally been raised about the influence of a slip sometimes occurring at a Cadweld splice at high stress levels. This project included only a sampling study, three beams with Cadweld splices of #18 bars, two with both bars spliced at the same cross section and one of

*Part of the concrete resistance is probably lost but more than replaced by the greater strength of the spiral or ties.

a single splice opposite a continuous bar. The staggering of these splices is recommended, just as with lap splices.

These Cadweld splices were made by inexperienced personnel in beams the same size (27-in. depth) as those used for the lap splices. All three beams failed in flexure at 99 percent to 103 percent of their computed moment capacity based on strain compatibility. When concrete was broken off the splices after the test, it was observed in one beam (18S-14C) having two splices there was a 0.03 in. space at one end of one Cadweld splice sleeve which indicated the amount of creep slip of the bar at that end of the sleeve. However, this slip at one end seemed to average in with the normal stretch within the sleeve and adjacent bar, to permit the beam to develop 103 percent of the computed moment capacity. Evidently such a local slip is not significant under these conditions, that is, in a beam 27 in. deep (maximum $f_s = 76.5$ ksi, $\epsilon_s = 0.014$ micro-inches).

Maximum crack widths for the #18 bar with the Cadweld splice presented essentially the same problem as with the #18 lap splice.

The Cadweld sleeve encroaches into the bar cover by 0.62 in. Presumably ties could be placed beyond the splices and tie thickness then could be deducted to give the net encroachment on the cover requirements.

CONCLUSIONS AND RECOMMENDATIONS

Adequate design rules for tension lap splices have been developed which, for the first time, reflect both the cover over the splice and the lateral clear spacing of splices. These design rules may also be applied to #14 and #18 bar lap splices which to date have been prohibited.

Transverse ties (or spirals) are desirable over all large bar splices and tentative recommendations have been made as to their strength evaluation in order to shorten splices. Ties are specially recommended for #14 bar lap splices (and are desirable for #11 where placement is feasible); they should be required for all #18 bar splices. Crack widths with #18 bars of Grade 60 are larger than with smaller bars and this is particularly true with splices, whether lapped or of Cadweld type, and probably also with any tension bar cut off outside a compression region.

Design Recommendations--Tensile Splices

$$\text{Grade 60 bars, } L_{s60} = 100D^2 \left(\frac{1}{S'} + \frac{1}{2C} \right) \geq 100D^2(1.5/S') \quad (3)$$

$$\text{Grade 40 bars, } L_{s40} = 57D^2 \left(\frac{1}{S'} + \frac{1}{2C} \right) \geq 57D^2(1.5/S') \quad (5)$$

No splice length less than 12 in.

<u>Given Conditions</u>	<u>Modifications</u>
$f'_c = 3000$ psi	For other f'_c , multiply L_s by $\sqrt{3000/f'_c}$
Concrete weight approx. 145 pcf	For lightweight concrete increase L_s as tensile strength drops
Other than top bars	For "top bar" splices multiply L_s by 1/0.6
Develop ductility beyond f_y	Strength collapsing at f_y not acceptable. Note strength not linearly proportional to L_s

<u>Special Cases</u>	<u>Modifications</u>
f_y at one end kf_y at other end }	Multiply L_s by $(1+k)/2$
f_y on D_1 at one end kf_y on D_2 at other end }	Multiply L_s by $(D_1^2 + kD_2^2)/(2D^2)$ Example: $L_{s60} = 50(D_1^2 + kD_2^2) \left(\frac{1}{S'} + \frac{1}{2C} \right)$
Staggered splices	Take $S' = 2S - 3D$, where S is bar spacing and $2S$ the splice spacing
Interior wall splices with f_y and kf_y	Multiply by $0.83(1+k)/2$ to give: $L_{s60w} = 42D^2(1+k) \left(\frac{1}{S'} + \frac{1}{2C} \right) \quad (4)$ $L_{s40w} = 24D^2(1+k) \left(\frac{1}{S'} + \frac{1}{2C} \right)$

Tentative Design Recommendations

- With transverse steel (ties or spirals)
- f_{st} can be assigned to ties if

$$A_v f_{yt} = 0.26 f_{st} D^2 (1 + 2S'/C)$$
 - With A_v multiply L_s by $(f_y - f_{st})/f_y$

PART B - SPECIMENS AND ANALYSIS

SPECIMENS AND TESTING

#11 Bar Splices

Nine specimens containing #11 bar splices were made to round out the information on splices for retaining walls already included in Report 113-2. The 32 members tested at that time left unanswered questions about the transition from face split to face-and-side split, the strength of the V-type failure, and the possible avoidance in a wall of the weaker face-and-side split mode.

The specimen details are recorded in Fig. 6 and Table 1. Six specimens, SP-31 to SP-36, each contained a single #11 bar splice centered on the width, modeling very widely spaced splices. The percentage of the main reinforcement was kept close to 0.62 percent and the overall thickness not less than the 12 in. minimum for a typical retaining wall stem with #11 bars. Splice length and bar cover were varied. The other three specimens had multiple splices, as shown.

Specimens were made from high-early strength cement (Type III) and Colorado River sand and gravel (1.5 in. maximum), using a water-cement ratio of approximately 6.6 gallons per sack. The several steel stress-strain curves are shown in Fig. 7 and the table in this figure indicates the beams in which each was used. Specimens were usually tested at 7 to 10 days of age.

The specimens were tested on their sides (Fig. 6a), as in the earlier series, by incremental loads to failure, with records of crack progress marked on the members and recorded by photographs. The splices were in a variable moment zone. Strains at several points along the splice bars were recorded, as well as surface concrete strains.

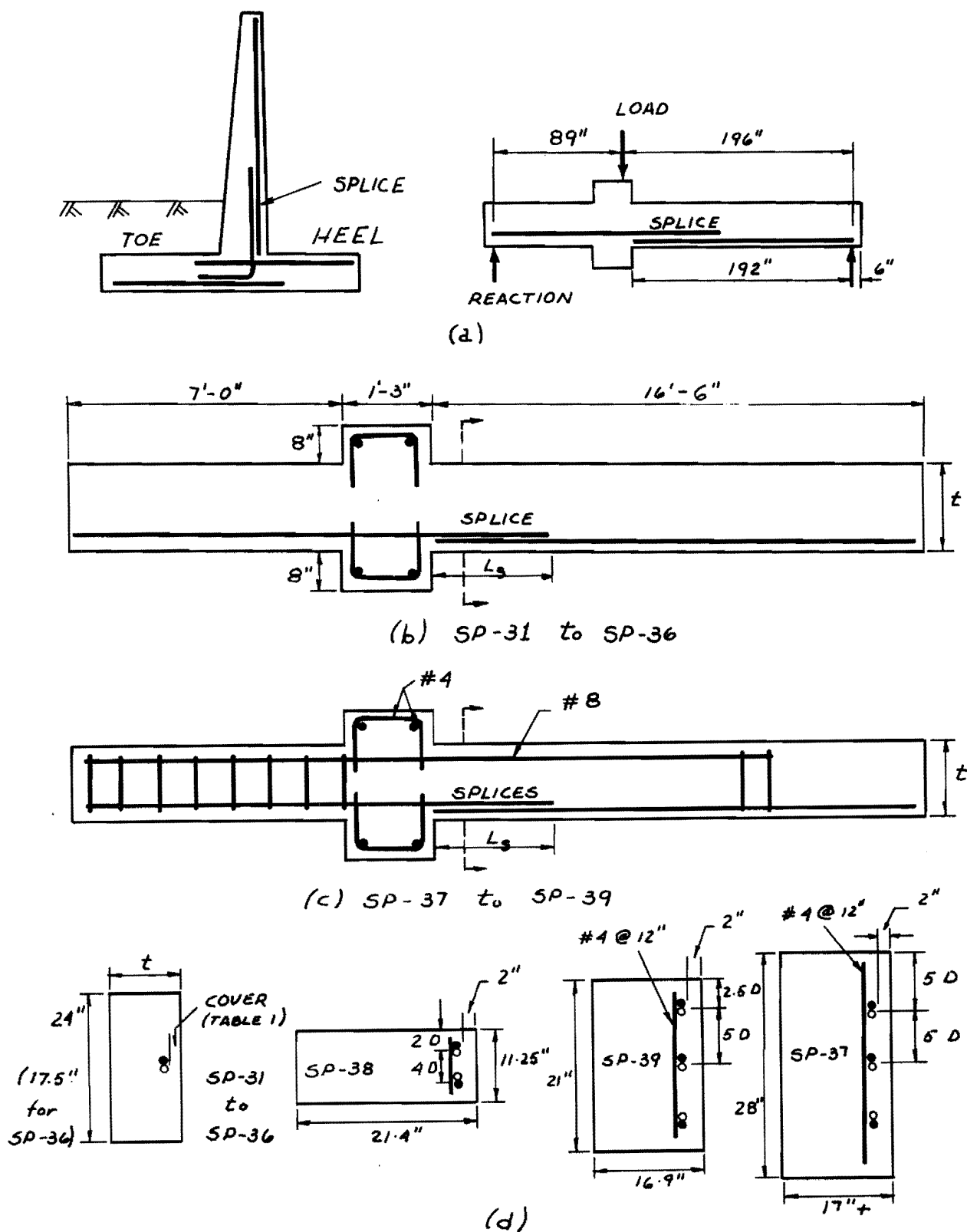




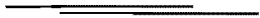
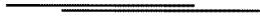
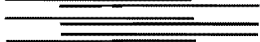
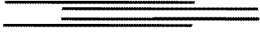
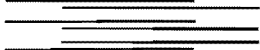


Fig. 6. Specimens with #11 bar splices.
 (a) Prototype and test specimen.
 (b, c) Specimen layouts.
 (d) Cross sections, all symmetrical.

TABLE 1. DETAILS OF #11 BAR SPECIMENS

Beam No.	b in.	t in.	S in.	C in.	L _s in.	f' _c psi	f _y ksi	Bar Arrangement
SP 31	24.00	12.00	24.00	1.25 ⁺	65.0	3960	67.5	
SP 32	24.00	12.25	24.00	1.25	50.0	3280	67.5	
SP 33	24.00	11.88	24.00	0.75	55.0	3360	67.5	
SP 34	24.00	12.00	24.00	0.75	36.0	3280	67.5	
SP 35	24.00	13.25	24.00	2.00	20.0	3310	67.5	
SP 36	17.50	17.25	17.50	2.00	24.0	3440	67.5	
SP 37	28.00	17.13	7.00	2.00	45.0	3260	67.5	
SP 38	11.25	21.38	5.62	2.00	40.0	2970	67.5	
SP 39	21.00	16.88	7.00	2.00	45.0	3120	71.7*	

⁺Average. Casting error caused $\pm 3/16$ " variation.

*Flat yield plateau.

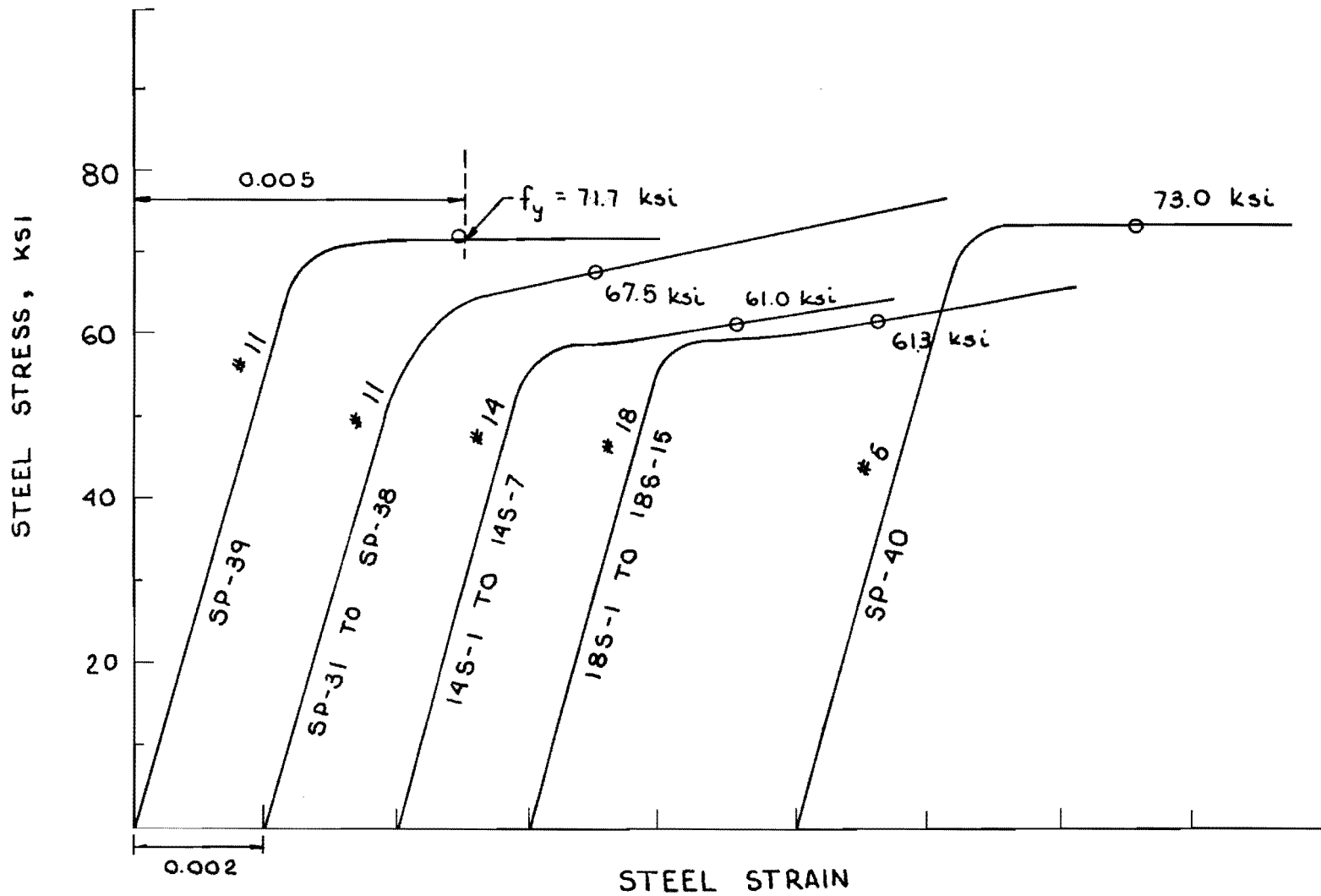


Fig. 7. Stress-strain curves for A-432 steels used.

#14 and #18 Bar Splices

Although of different dimensions the 7 - #14 and the 15 - #18 splice beams were otherwise similar, each with the splice located in a constant moment region when tested. The specimen details are given in Figs. 8 and 9, and the dimensions and properties in Tables 2 and 3. Two #18 splice beams contained a single splice and one continuous bar, indicated at the end of the numbering code by letter S. A letter C likewise indicates Cadweld splices instead of the lap splices. Spirals, where used around the splices, were extended two pitches each way beyond the lap.

The spliced bars were A432 deformed bars with the stress-strain curves shown in Fig. 7. Transverse reinforcement was of intermediate grade steel with the f_{yt} noted in Tables 2 and 3. Spirals were made from plain 1/4-in. diameter bars for #14 and 3/8-in. for #18 bar specimens.

Electrical resistance strain gages were mounted on one or more splices in each beam and occasionally on the transverse reinforcement around the splices.

Ready-mixed concrete, as for the #11 bar specimens, was used with a water-cement ratio of about 6.2 gallons per sack, cement factor 4.5 sacks per cubic yard, and slump 3 in. The specimens were cast on their side, moist cured for 5 days, and tested, still on their side, after 7 days.

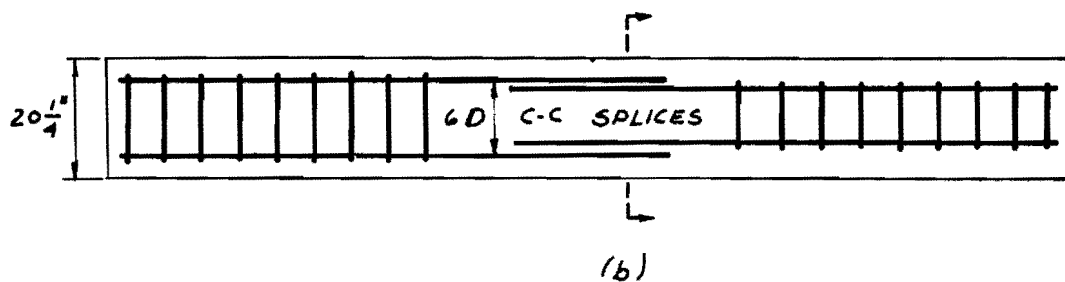
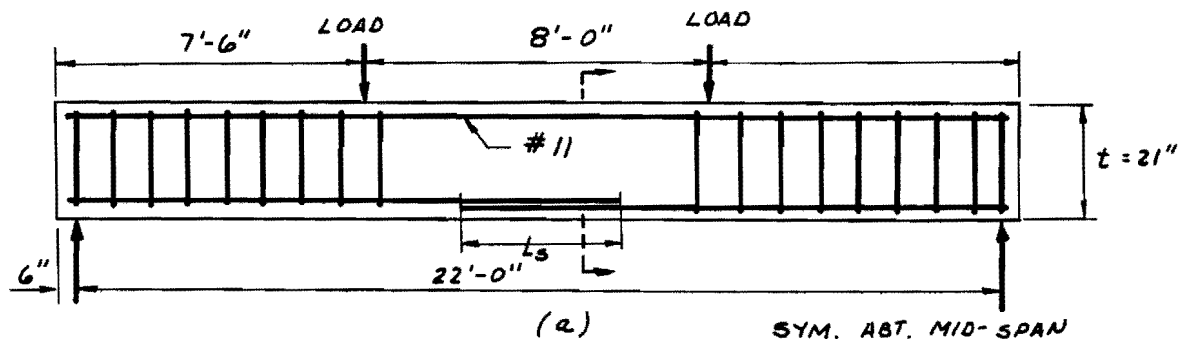
The Cadweld splices were made by inexperienced personnel, but following the manufacturer's instructions and a demonstration by the manufacturer's representative.

#5 Bar Splices

One specimen with #5 bar lap splices (Fig. 10) was modeled after the #18 bar beam 18S-12. In terms of bar diameter, all dimensions except for a small difference in splice length were identical. This length was 24D for the #5 splice and 26.7D for the #18. This specimen was used to check whether stress similitude can be obtained by proportioning in terms of bar diameters.

Testing

The typical test setup for #14 and #18 bars is sketched in Fig. 11, and for the #11 bars was somewhat similar as indicated in Fig. 6a. Each



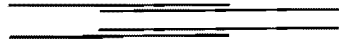

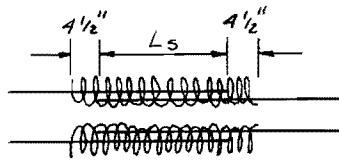
Section Beam No. Transverse Reinforcement

	14S-1	None
	14S-2	19 #2 U at 2-3/4 in.
	14S-3	19 #2 U alternating 1 and 2 at 2-1/4 in.
	14S-7	20 #3 U at 2-1/4 in.
	14S-4	#2 spiral at 2-1/4 in. pitch, 5-1/4 in. internal diameter
	14S-5	#2 spiral at 2-1/4 in. pitch, 5-1/4 in. internal diameter
	14S-6	#2 spiral at 2-1/4 in. pitch, 5-1/4 in. internal diameter

Fig. 8. Specimens with #14 Bar splices.
 (a) Elevation
 (b) Plan
 (c) Cross sections, all symmetrical

TABLE 2. DETAILS OF #14 BAR SPECIMENS

D = 1.69 in. Splice spacing = 10.2 in. Clear cover (over bars) = 2.4 in. $f_y = 61.0$ ksi

Beam No.	b	t	L_s	f'_c	Transverse Reinforcement			Splice Bar Arrangement
					Type	a_v	f_{yt}	
14S1	20.50	21.00	45.0	2710	None	0	-	
14S2	20.50	21.00	54.0	3345	U-stirrups	0.95	51.0	
14S3	20.38	21.00	30.0	3020	U-stirrups	0.95	51.0	
14S7	20.50	21.25	45.0	3700	U-stirrups	2.20	62.0	
14S4	20.50	21.00	30.0	3200	Spirals (eccentric)	1.47	62.0	
14S5	20.50	21.00	45.0	3390	Spirals (eccentric)	2.20	62.0	
14S6	20.50	21.13	36.0	3570	Spirals (eccentric)	1.76	62.0	

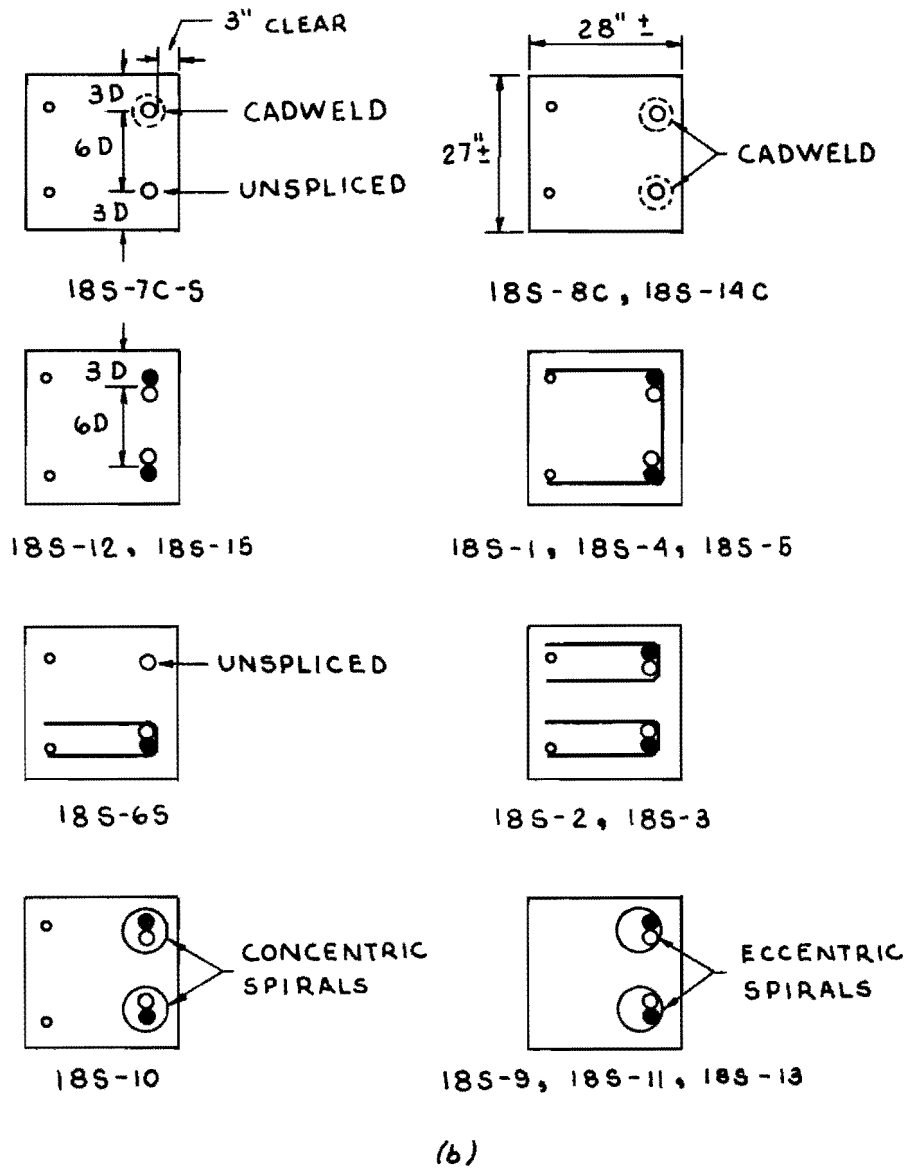
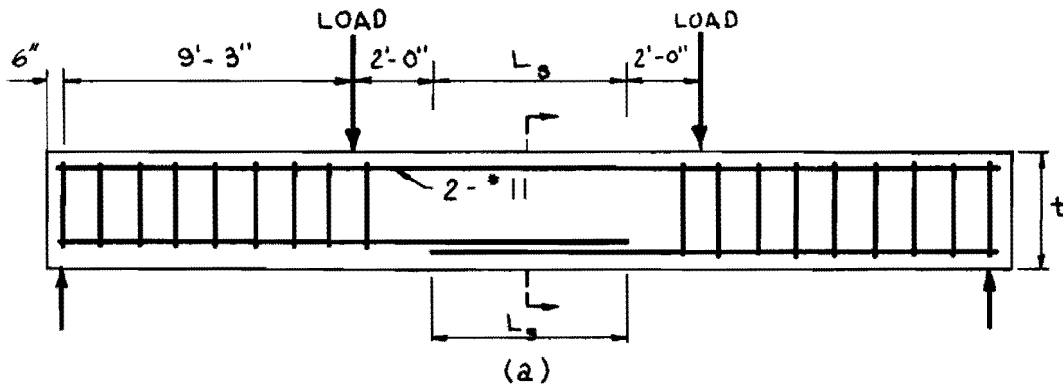
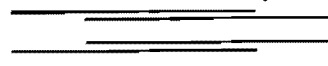
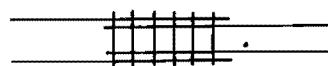
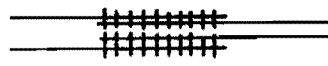
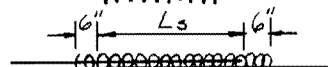
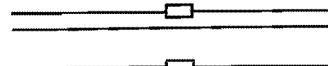


Fig. 9. Specimens with #18 bar splices.
 (a) Elevations
 (b) Cross sections

TABLE 3. DETAILS OF #18 BAR SPECIMENS

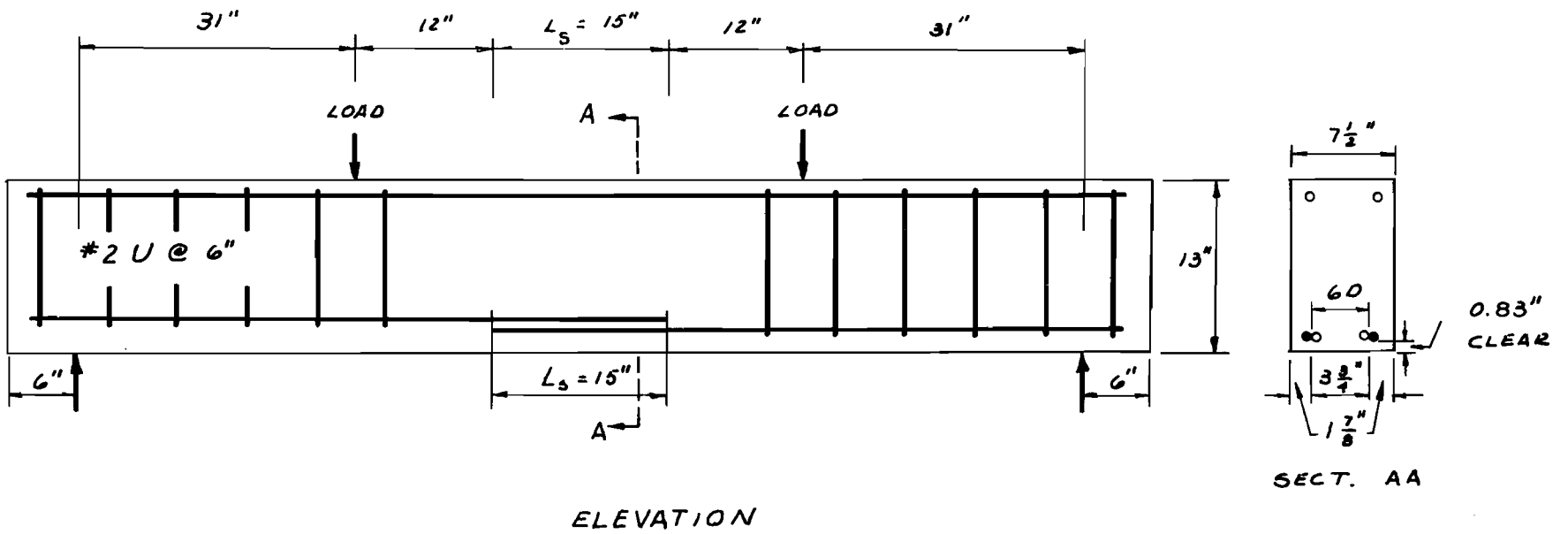
D = 2.25 in. Splice spacing c-c = 13.5 in. Clear cover (over bars) = 3.0 $f_y = 61.3$ ksi

Beam No.	b in.	t in.	L_s in.	f'_c psi	Transverse Reinforcement				Splice Bar Arrangement
					Type	A_v sq.in.	f_{yt} ksi	Details	
18S12	27.25	28.00	60.0	3160	None	-	-	-	[]
18S15	27.00	28.10	98.0	2860	None	-	-	-	
18S1	27.13	28.13	72.0	2710	U Stirrups	1.43	56.6	13 No. #3] ]
18S4	27.20	28.20	60.0	3940	"	4.00	50.5	20 No. #4	
18S5	27.25	28.50	72.0	4050	"	4.80	50.5	24 No. #4	
18S2	27.13	28.13	60.0	2620	Hairpins	2.86	56.6	13 pair #3] ]
18S3	27.13	28.25	72.0	4650	"	1.30	44.5	13 pair #2	
+18S6S	27.13	28.25	72.0	3520	"	5.06	56.6	23 No. #3	
18S9	27.25	28.25	60.0	3010	Spirals	4.40	60.0	3/8", 3" pitch] ]
**18S10	27.38	28.25	60.0	3190	"	4.40	60.0	3/8", 3" pitch	
18S11	27.25	28.50	60.0	3220	"	2.20	60.0	3/8", 6" pitch	
18S13	27.25	28.00	48.0	3400	"	3.52	60.0	3/8", 3" pitch	
+18S7C-S	27.13	28.25	Cadweld	3820	-	-	-	-] ]
18S8C	27.13	28.25	"	3700	-	-	-	-	
18S14C	27.25	28.13	"	3010	-	-	-	-	

*Internal diameter of spiral = 6.25 in.

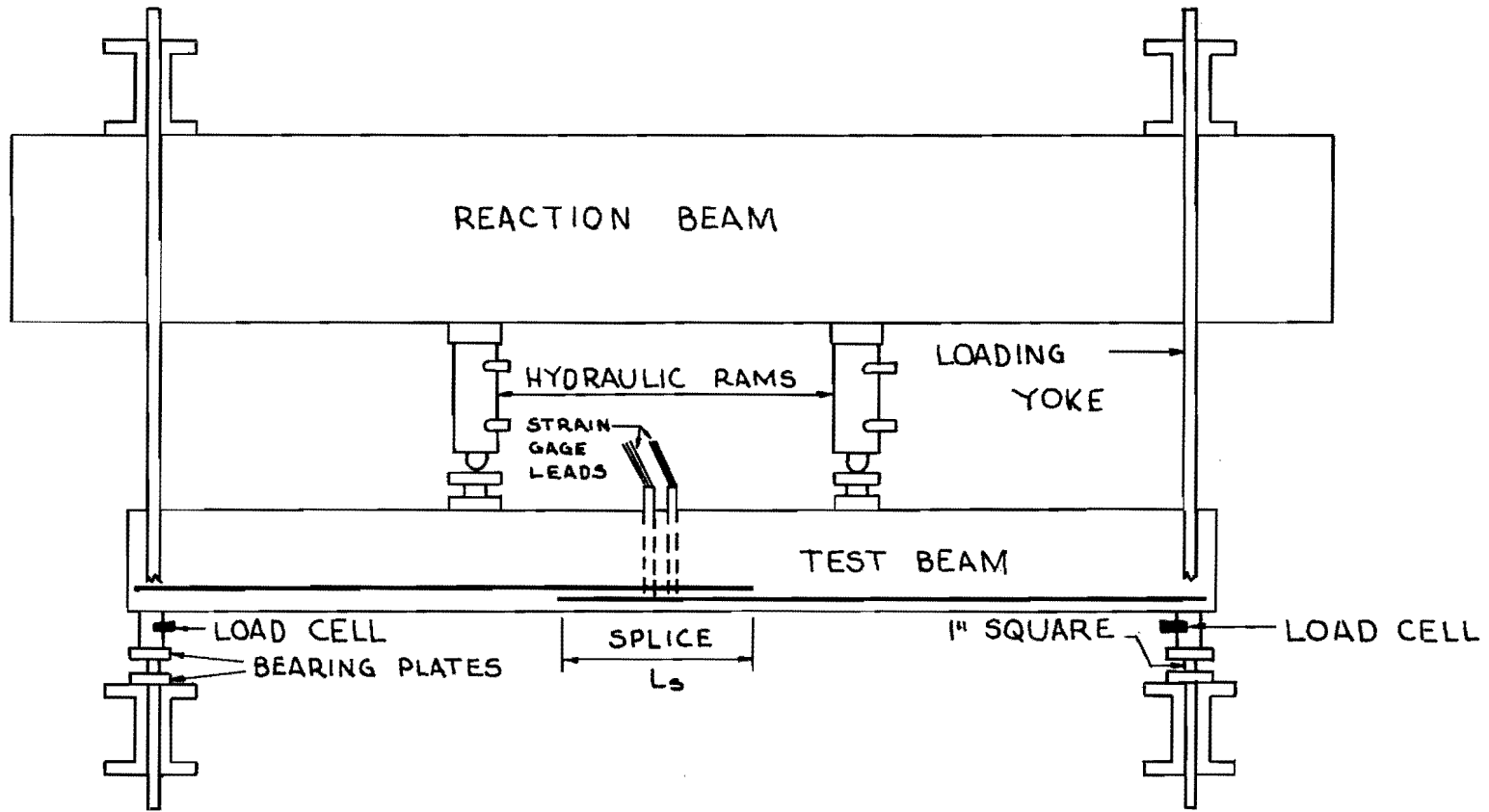
+one spliced bar and one unspliced bar

**Concentric spiral



$$f'_c = 3220 \text{ psi} \quad f_y = 73.0 \text{ ksi}$$

Fig. 10. Splice beam SP-40 with #5 bar splices.



(#18S series same except load cells omitted)

Fig. 11. Test setup for #14S series, plan view.

specimen was tested on its side, supported vertically on 7 in.-diameter rollers and horizontally against steel yoke reactions at each end. Two hydraulic jacks loaded the #14 and #18 splice members and produced a constant moment over a length at least two beam depths greater than the splice length. A single jack loading on the #11 splice members produced a varying moment over the splice length. Load was monitored by a calibrated jack pressure gage in the #18 bar series and by load cells in the #11 and #14 bar series. Incremented loading was applied to failure, with cracks marked after each increment.

Widths of surface cracks on the tension face were measured in beams 18S-12, 18S-13, 18S-14C, in all of #14 bar beams, and in the 9 - #11 bar specimens. The test results and calculated values are given in Table 4. From beams that failed by splitting, the concrete cover over the bars was later pried off to inspect the splice, the failure surface, and the end slip.

GENERAL BEHAVIOR OF SPLICES

V-Type Failure

Specimens SP-31 through SP-35 with single #11 splices were wide members, to force a V-type of failure. With more typical types of splitting failure thus avoided, the behavior and strength must be considered to represent an upper bound or limiting situation.

Flexural cracks appeared first at the higher stressed end of the splice adjacent to the loading stub and progressed along the splice as the load increased, with the crack at the lower stressed end appearing earlier than the neighboring flexural cracks. Localized shearing problems across the splice became evident, first at around 50 to 60 percent of ultimate load, with the initiation of short diagonal cracks on the tension face. These developed gradually into a series all along the splice, as shown in Fig. 12a, building up a zone of local weakness. A violent type failure occurred by fracture of the concrete in a splitting type failure over the splice, making it easy to expose the V-type channel of Fig. 12b. The splice shown was 39D long with a clear cover of 0.75 in. It reached a satisfactory stress level of around 75 ksi, but did not quite develop a flexural failure. The shorter

TABLE 4. DATA AND COMPUTED VALUES

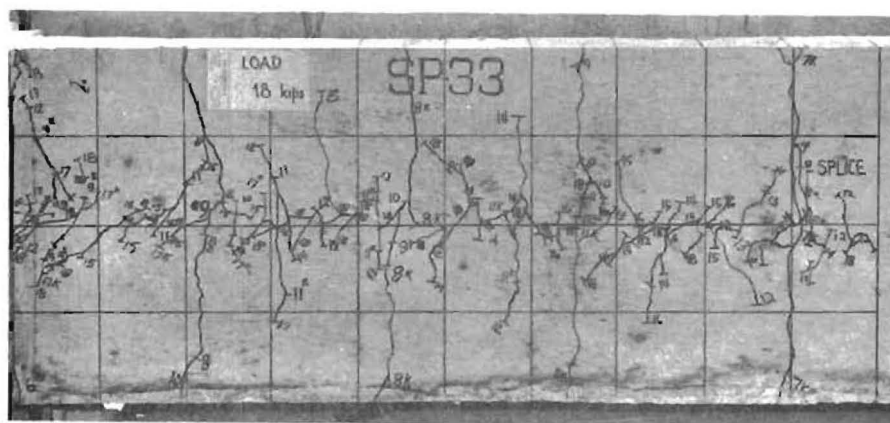
Beam No.	f' _c psi	f _y ksi	L _s in.	S in.	C in.	A _v sq.in.	f _{yt} ksi	f* _{su}	Máx. Bar Strain	Failure
SP-31	3960	67.5	65	24.00	1.25 ⁺	-	-	82.7	0.00284	Flexure
SP-32	3280	67.5	50	24.00	1.25	-	-	72.5	0.00846	VS
SP-33	3360	67.5	55	24.00	0.75	-	-	75.5	0.00791	VS
SP-34	3280	67.5	36	24.00	0.75	-	-	54.5	0.00198	VS
SP-35	3310	67.5	20	24.00	2.00	-	-	38.4	0.00133	VS
SP-36	3440	67.5	24	17.50	2.00	-	-	47.5	0.00161	VS
SP-37	3260	67.5	45	7.00	2.00	-	-	69.2	0.00727	Fig. 15c
SP-38	2970	67.5	40	5.62	2.00	-	-	43.5	0.00150	SS & FS
SP-39	3120	71.7	45	7.00	2.00	-	-	51.1	0.00214	FS
SP-40	3220	73.0	15	3.75	0.83	-	-	43.1	-	FS
14S1	2710	61.0	45	10.2	2.38	-	-	45.6	0.00206	FS
18S12	3160	67.5	60	13.5	3.00	-	-	45.2	0.00158	FS
18S15	2860	67.5	93	13.5	2.63	-	-	51.6	0.00178	FS
<u>STIRRUPS</u>										
14S2	3345	61.0	54	10.2	2.38	0.95	51.0	59.5	0.00241	FS
14S3	3020	61.0	30	10.2	2.38	0.95	51.0	39.0	0.00156	FS
14S7	3700	61.0	45	10.2	2.38	2.20	62.0	66.5	0.00888	Flexure
18S1	2710	67.5	72	13.5	3.00	1.43	56.6	65.6	0.00752	FS
18S4	3940	67.5	60	13.5	3.00	4.00	50.5	66.0	0.00810	FS
18S5	4050	67.5	72	13.5	3.00	4.80	50.5	71.0	0.01192	Flexure
<u>HAIRPINS</u>										
18S2	2620	67.5	60	13.5	3.00	2.86	56.6	52.6	0.00189	FS
18S3	4650	67.5	72	13.5	3.00	1.30	43.0	59.5	0.00205	FS
18S6S	3520	67.5	72	13.5	3.00	5.06	56.6	68.2	0.00910	Flexure
<u>SPIRALS</u>										
14S4	3200	61.0	30	10.2	2.38	1.47	62.0	50.0	0.00225	FS
14S5	3390	61.0	45	10.2	2.38	2.20	62.0	69.6	0.00662	Flexure
14S6	3570	61.0	36	10.2	2.38	1.76	62.0	60.0	0.00550	FS
18S9	3010	67.5	60	13.5	3.00	4.40	60.0	70.4	0.01150	Flexure
18S10	3190	67.5	60	13.5	3.00	4.40	60.0	74.2	0.01336	Flexure
18S11	3220	67.5	60	13.5	3.00	2.20	60.0	62.2	0.00240	FS
18S13	3400	67.5	48	13.5	3.00	3.52	60.0	59.4	0.00260	FS
<u>CADWELDS</u>										
18S7C-S	3820	67.5	-	13.5	3.00	-	-	70.5	0.00994	Shear-comp.**
18S8C	3700	67.5	-	13.5	3.00	-	-	67.5	0.01008	Flexure
18S14C	3010	67.5	-	13.5	3.00	-	-	67.8	0.01432	Flexure

SS - Side split; FS - Face-and-side split; VS - V-split.

⁺ Average cover.

$$* f_{su} = M_u / (0.9d A_s)$$

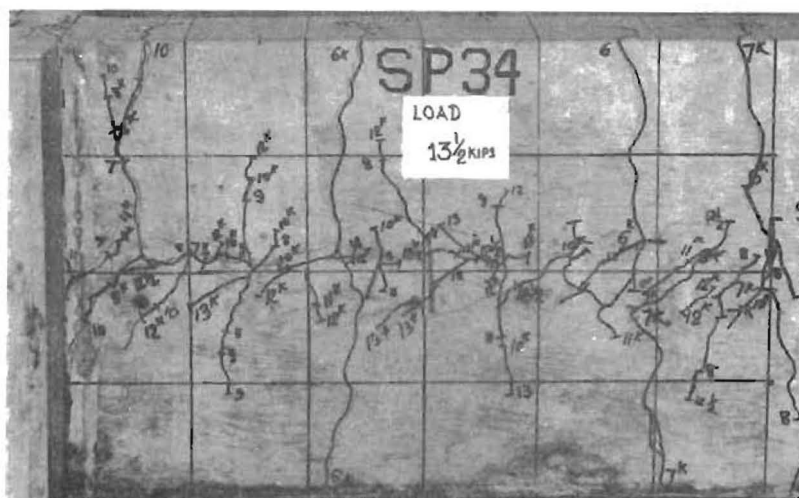
** Not related to splice.



(a) Crack pattern on the tension face at 97% ultimate, $L_s = 55$ in.



(b) The failed surface, V-type.



(c) Cracks on tension face as beam was failing, $L_s = 36$ in.

Fig. 12. V-type failures, #11 bar splices.

25.5D splice of SP-34 shown in Fig. 12c behaved similarly and reached nearly a 55 ksi stress level.

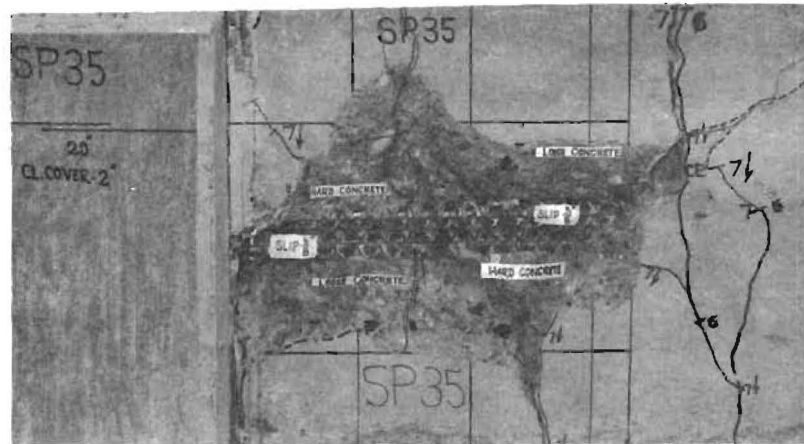
When cover was increased to 2 in. clear over a shorter (14.2D) splice, the local diagonal cracking reached farther from the bars (Fig. 13a), the V-channel was wide, and some transverse bending over the whole beam section seemed to be indicated by the final cracks shown in Fig. 13b and 13c. Failure appeared to have developed from the overall diagonal crack running in Fig. 13b from upper right to lower left and wrapping around the side and compression face of the beam (Fig. 13c) in combination with the longitudinal splitting.

Variations from the Side Split Mode of Failure

The earlier portion of the investigation (Research Report 113-2) showed clearly two types of failures. For closely spaced bars (splice spacings less than $4D$ on centers with 2 in. clear cover), a side split totally across the beam separated the cover concrete from the beam proper, with little or no longitudinal splitting through the cover. At these close spacings an individual splice strength is the same whether it is alone or parallel with three or four other splices in one beam.

At wider spacings such as $5D$ or $6D$, the final failure was also by loss of the cover concrete, but with an important difference. Longitudinal cracks gradually developed over each splice and when these cracks finally extended over the splice length the failure was complete and sudden. It was thought then (Report 113-2) that the shoulder or corner elements (Fig. 14a) were weaker and triggered the longitudinal splitting. It appears now that the sequence is a gradually developing longitudinal split which permits the formation of an increasing length of corner element with its lesser resistance. This process leads finally to a sudden and rather violent failure. As reported then, a given concrete width failing in this manner is less strong than would be predicted by extrapolating from side split failure strengths.

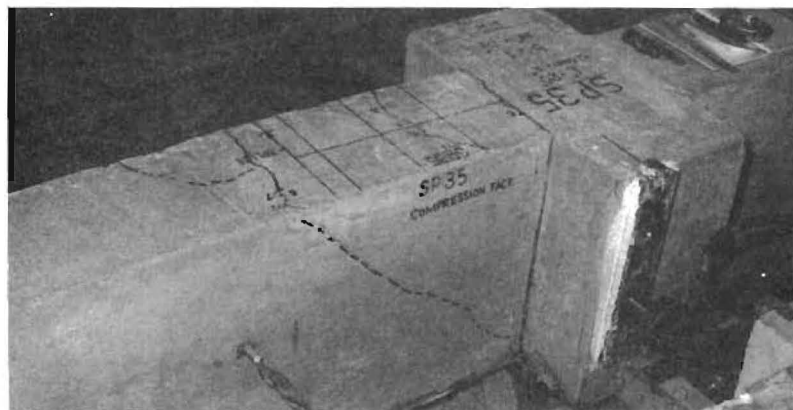
A transition case developed in beam SP-38 which had two splices spaced $4D$ on centers with clear cover of 2 in. A longitudinal split occurred over the upper splice (in Fig. 14b) and the failure over the other splice was definitely a side split failure, as the exposed failure surface in Fig. 14c clearly indicates.



(a) Loose concrete removed.

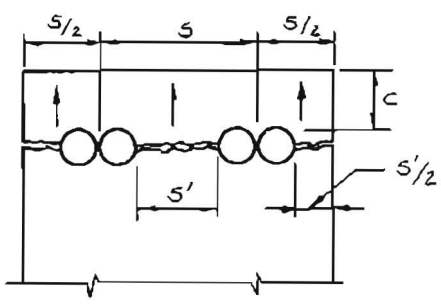


(b) Dashed lines mark cracks added at ultimate.

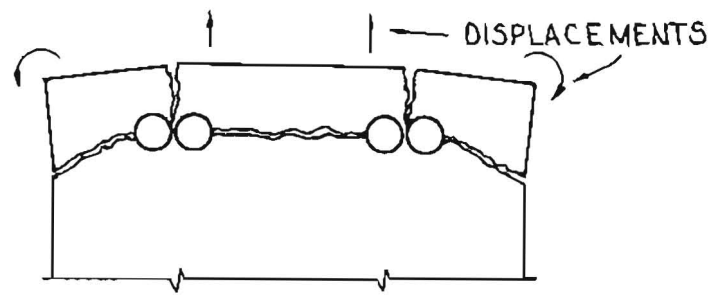


(c) Ultimate cracks on side and compression face.

Fig. 13. V-type failure, #11 splice, $L_s = 20$ in.

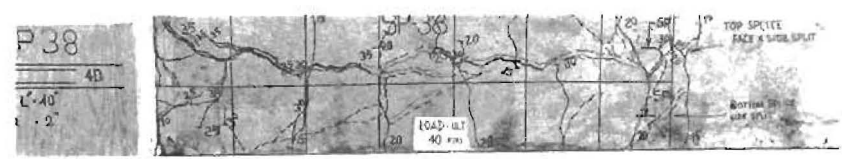


Side split

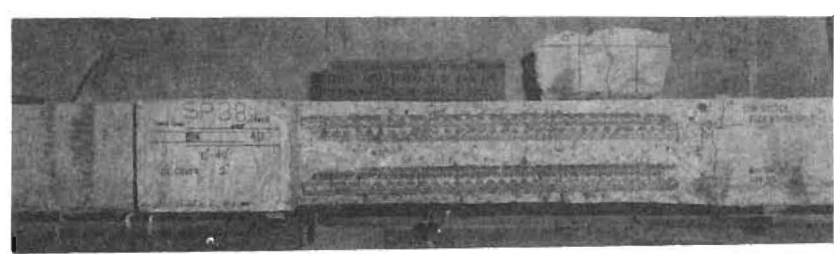


Face-and-side split

(a) Types of failure.



(b) Note face split top splice only.



(c) Failure surface.

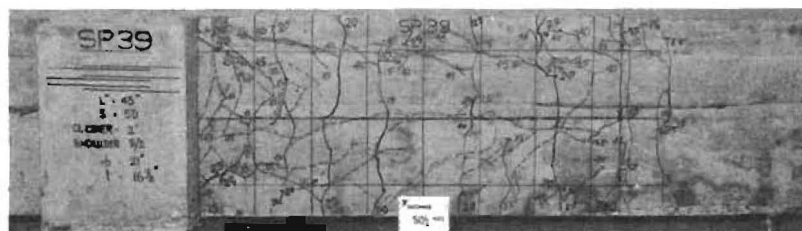
Fig. 14. Mixed face-and-side split (upper splice) and side split (lower splice).

It was theorized in Report 113-2 that a wall-type structure might prevent the formation of the weak corner element which tended to rotate about a longitudinal axis because of its eccentric loading. Without this rotation wall splices might be more highly rated. Beams SP-37 and SP-39 related to this question, each containing 3 splices at the same 5D center spacings, SP-39 with a half space at each edge and SP-37 a 5D edge distance. Beam SP-39 failed with one definite face split and two partial face splits (Fig. 15a, b) resulting in total loss of the cover concrete. Beam SP-37 failed after much tension surface cracking (Fig. 15c) with the edge shoulders intact except for flexural cracks. The strength was increased 37 percent, for a width increase of 33 percent, but how much of this is due to the half V-type failure at the outside splices and how much to the lack of a face-and-side split there is not established. Presumably a lesser width permitting a side split but with shoulders stiff enough to avoid the face-and-side split failure would also give an improved strength but less than that of this specimen. Definitely, a wall having the end bar unspliced or spliced at a different height will provide splice strengths for interior bar splices above those of equal spaced splices in beams where a face-and-side split failure pattern is possible.

Splices of #14 and #18 Bars

A spacing of 6D was adopted for all the very large bar tests. Six specimens combining lap lengths and transverse reinforcement were adequate to bring flexural failure, including secondary failure in compression, at a bar stress over 68 ksi and in 3 cases over 70 ksi, well beyond the yield point. In the other specimens the splices failed and the expected face-and-side split occurred. The cracking pattern was similar to that observed in other symmetrical splice beams under constant moment loading. Possibly the larger beam size directed attention to a closer observation of crack behavior and the presence of spirals or stirrups in many specimens possibly resulted in some modifications in the behavior pattern.

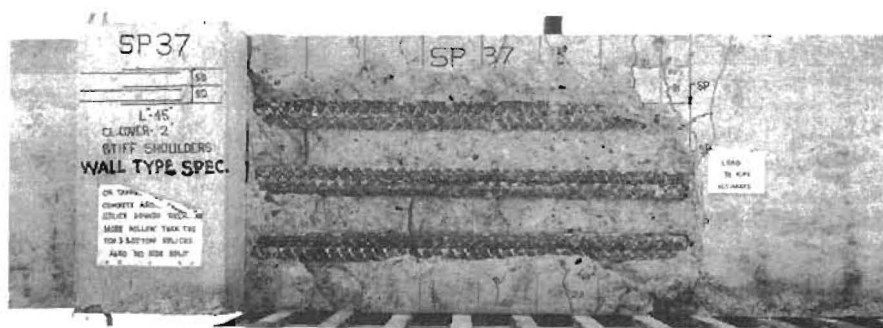
Inclined secondary cracks caused by differential strains in the spliced bars began to appear at the splice ends at 50 to 60 percent of ultimate, their orientation quadrant dependent upon the bar arrangement as indicated in Fig. 16. These appear to have been caused by the greater slip



(a) Upper full face split and two lower less pronounced.



(b) Failure surface.



(c) Failure surface when edge distance equals spacing.

Fig. 15. Triple #11 splice, $L_s = 45$ in., $S' = 3D$.

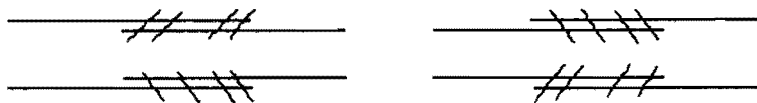


Fig. 16. Secondary cracking pattern in tension splices.

of the cut end of the bar relative to the continuing bar. Beams with stirrups or spirals around the splices sustained greater load and developed more secondary cracks.

Longitudinal splitting appeared at 70 to 80 percent of the ultimate load, initiating from both flexural and secondary diagonal cracks, but not necessarily at the axis of the splice. None but flexural cracks showed on the sides of the beam until the shoulders broke off in the final failure (Fig. 17a). These final cracks on the side of the beam were typically a series of diagonal cracks rather than cracks parallel to the bars.

With stirrups or spirals, ultimate failure was more gradual and less violent, but resulted in the same wide longitudinal splitting over the splice length and the subsequent shoulder failure. A failure with spiral at 3 in. pitch is shown in Fig. 17b, c and with a 6 in. pitch in Fig. 18a. A failure with ties is shown in Fig. 18b, c.

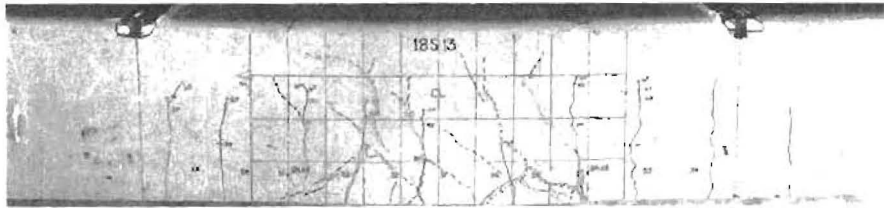
In general splices with ties were stronger than those without ties, and those with spirals were some 10 percent stronger than the ones with ties. All spirals were eccentrically placed with respect to the splice (Figs. 8 and 9), except in 18S-10. This centered spiral showed a little higher strength than the comparable eccentric one, but this is inconclusive because both specimens failed in flexure.

Splices of #5 Bars

The single small bar splices (SP-40), modeled after beam 18S-12, cracked and failed in a similar manner to the large beam. A smaller number of flexural and other cracks developed in the small beam but the pattern was similar (Fig. 18d) and the strength comparison was closely in line.

Cadweld Splices

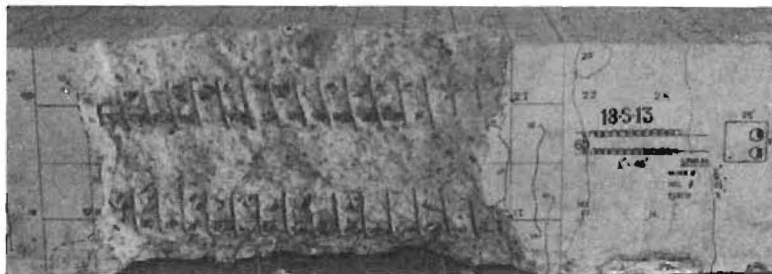
The Cadweld splices were adequately discussed in Part A, except as to the crack patterns which are shown in Fig. 19. The Cadweld location is



(a) Side cracking. The dashed cracks opened only at ultimate.



(b) Tension face cracking.



(c) Failure surface.

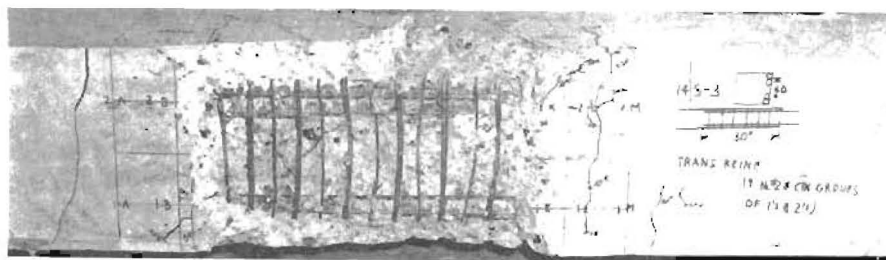
Fig. 17. 48 in. lap splice of #18 with 3/8 in. spirals at 3 in.



(a) Failure #18 splice with 3/8 in. spiral
at 6 in., $L_s = 60$ in.



(b) Failure #14 splice with 19 #2 U in $L_s = 30$ in.

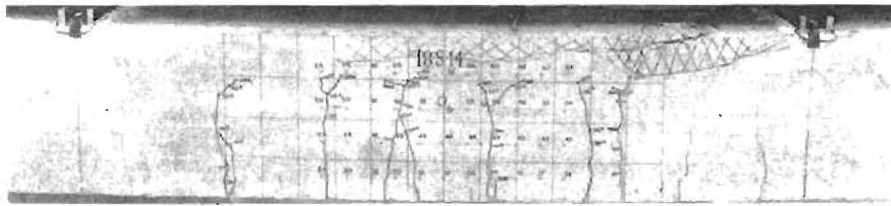


(c) Failure surface of specimen in (b).

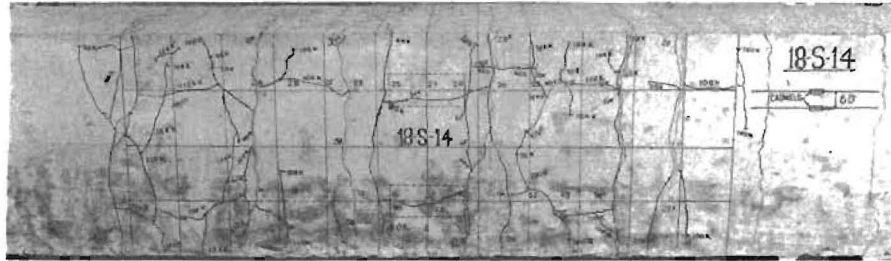


(d) Failure #5 splice (no transverse steel),
 $L_s = 15.1$ in.

Fig. 18. Wide ranges of splice bar sizes gave same failure pattern.



(a) Side of beam showing flexural crushing.



(b) Cracking on tension face. Splices shown dotted.



(c) Side of beam. Shear compression failure from loading arm.



(d) Tension face. Note lower bar is continuous.

Fig. 19. Cadweld splices of #18 bars.

shown dotted on these views. These figures show clearly that at high stresses with these covers (2.4 in. for #14 and 3 in. for #18) longitudinal cracks will develop over portions of unspliced bars and over the Cadweld splice also.

ANALYSIS OF RESULTS

Distribution of Bar Tension Along the Splice

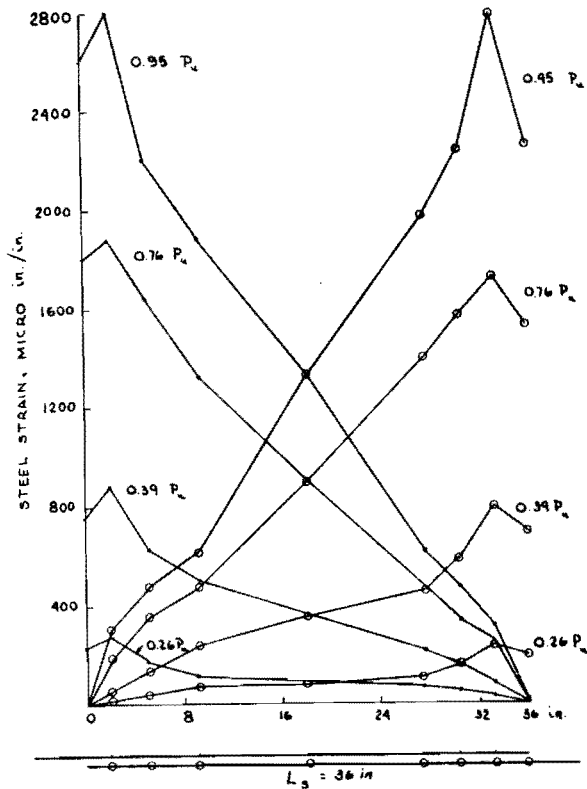
The distribution of tension along any of the spliced bars is similar to that recorded for the #11 bars in Report 113-2. Figure 20a,b shows, first, strains for beam 14S-6 (with a spiral around each splice) and then the corresponding stresses. The strains increase more at the splice ends near ultimate than do the stresses because the stress there is along the flattening portion of the stress-strain curve (Fig. 7). With one bar continuous and one spliced, beam 18S-6S with hairpins over the splice showed the stress distributions in Fig. 20c.

The assumption of linear stress distribution at ultimate is rather good, but it does not reflect the actual trend toward a more rapid increase near the cutoff end and a very inefficient region at the maximum stress range. It is surmised that the excessive shear distortions in the concrete between (and around) the bars has fractured some shear planes and shifted the normal resistance to a concentration of stress build-up near the bar end and a reduced amount on the continuing bar.

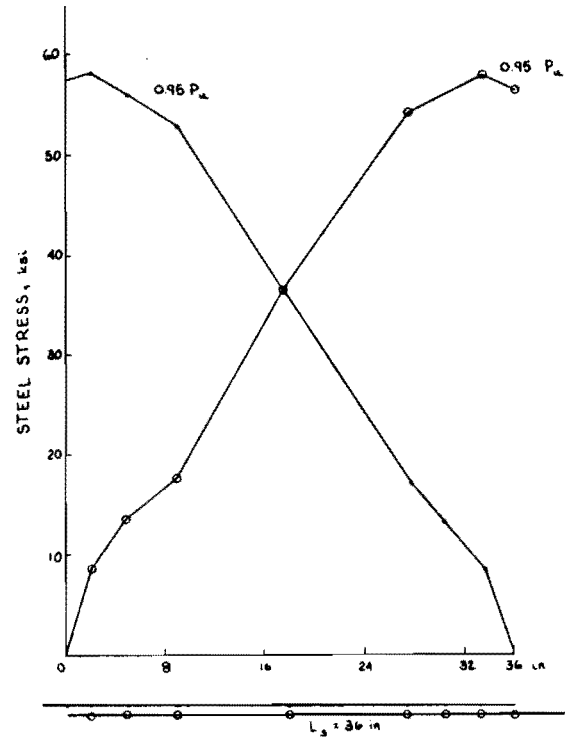
Feasibility of Lap Splicing of #14 and #18 Bars

Flexural failures (secondary compression) resulted in 4 of the #18 bar beams and 2 of the #14 bar beams, indicating that strength and ductility requirements can easily be met by lap splices. The complications related to crack widths have already been discussed adequately in Part A and are not treated further here.

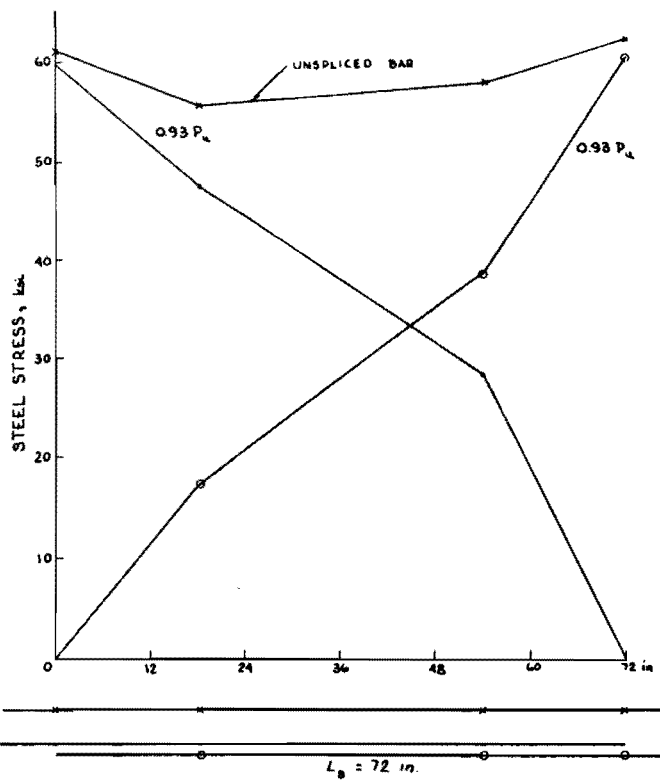
The combinations which operated successfully are given in Table 5. The maximum f_s tabulated is calculated as $f_{su} = M_u / (0.9dA_s)$ but the steel strain ϵ_s is a resistance strain gage observation which, because of the cracking pattern, could read below the real maximum where concrete acted in tension between flexural cracks.



(a)



(b)



(c)

Fig. 20. Steel strains and stresses along splices.

- (a) Strains in beam 14S-6 at various load levels. (Spiral around each splice, face-and-side split failure.)
- (b) Stresses in beam 14S-6.
- (c) Stresses in beam 18S-6S. (Hairpins around splice, flexural failure.)

TABLE 5. BEAMS FAILING IN FLEXURE

Beam	f'_c psi	f_y ksi	L_s in.	Transverse Reinf.			f_{su} ksi	ϵ_{su}
				Type	Size	Spcg.		
14S-5	3390	60.0	45	Spiral	1/4"	2.25"	69.6	0.00662
14S-7	3700	60.0	45	Stirrup	3/8	2.25	66.5	0.00882
18S-5	4050	60.5	72	Stirrup	#4	3.00	71.0	0.01192
18S-6S	3520	60.5	72	Hairpin	#3	3.12	68.2	0.00910
18S-9	3010	60.5	60	Spiral	3/8	3.00	70.4	0.01150
18S-10*	3190	60.5	60	Spiral*	3/8	3.00	74.2	0.01336

*Spirals centered on splices.

With a long flat yield plateau on the steel stress-strain curve, differential deformations near splice ends must ultimately deteriorate the resistance available there. It appears to the writers that a practical splice requirement ultimately will have to be stated in terms of something like the present idea of a stress capacity of $1.25f_y$ or, alternatively, a maximum strain of 0.008, or 0.0010, or some such limit. No such standard is even under discussion at this time. It should be noted that both f_{su} and ϵ_u values are not at a splice failure but are those necessary in these beams to produce complete flexural failure.

The splice design aspects for strength with these large bars are treated in the next section and appear not to need differentiation from smaller bars.

A Modified Approach to Splice Design

In Report 113-2 emphasis was placed on S/D , the ratio of splice spacing (center-to-center) to the bar diameter. Splice strength was greatly increased as this ratio increased. With a wider range of specimens, more bar sizes, and varying cover, the clear cover developed as even a more important variable than bar diameter. The cover controls the type of failure whether side-split, face-and-side split, or V-type. The clear space S' between two splices rather than center-to-center spacing S also seemed more

significant. The following study was therefore made on the basis of the ratio S'/C , clear spacing to clear cover, as the major variable.

Other variables are important, but, of these, only variations in f_y are presently clear enough to be considered separately. Splice length also is important, since splice strength does not double if the lap is doubled. Increasing bar diameter also requires an increased length, just as does increasing f_y . The treatment here suggested is not the final answer to the problem, but it constitutes an improvement over all previous formulations.

The use of S'/C permits some separation of the three failure modes shown in Fig. 21. The data from all available splice tests in the literature have been reanalyzed in Tables A.1 through A.3 in the Appendix and it was observed that failure types segregated as shown in Fig. 21d.

The Briceno studies, given in Report 113-2, had assumed that a splitting pressure existed around the bar equal to its bond stress and that the concrete was able to mobilize its splitting resistance uniformly over the splice length and over the beam width, at least in the side split failure case. The nonuniform steel stress gradients in Fig. 20b indicate that there must be some loss of efficiency near the ends of the splice, at least for a long splice. As Briceno indicated, the uniform resistance of the concrete laterally must change as one moves from the side split to the face-and-side split mode, although his distribution in this case may be questioned. With the V-split failure still other lateral distributions exist. With various ratios of clear cover to bar size it is suspected that the ratio of splitting pressure around the bar to the bond stress also varies in different splice situations.

The approach used here is to assume the splitting plane as the plane of the bars, recognize that the concrete across this splitting plane will be subjected to a tensile stress varying in magnitude both transversely and lengthwise of the splice, and assume that the ratio of this average ultimate splitting stress to the tensile splitting strength of the concrete is a function of the other variables. The actual total splitting stress is related to the total pull on the two lapped bars, but it is not known whether the radial component is equal to this pull (as Briceno used it), or is more, or less.

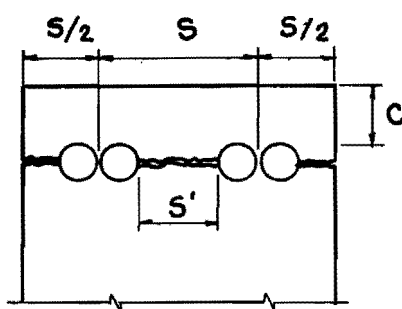
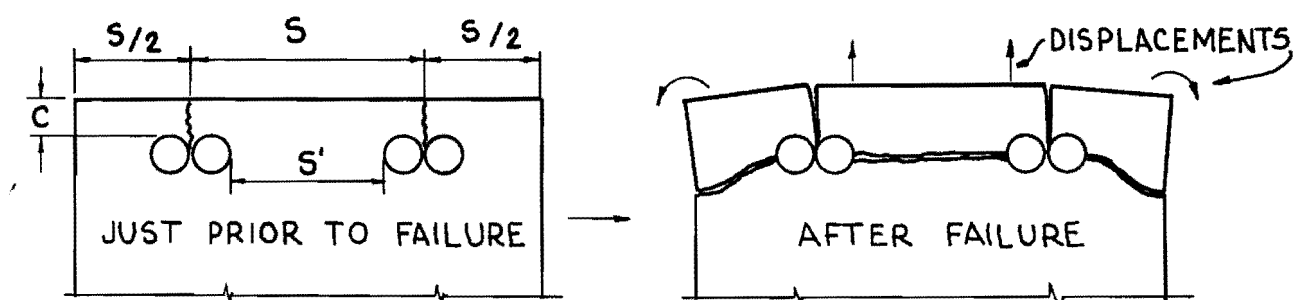
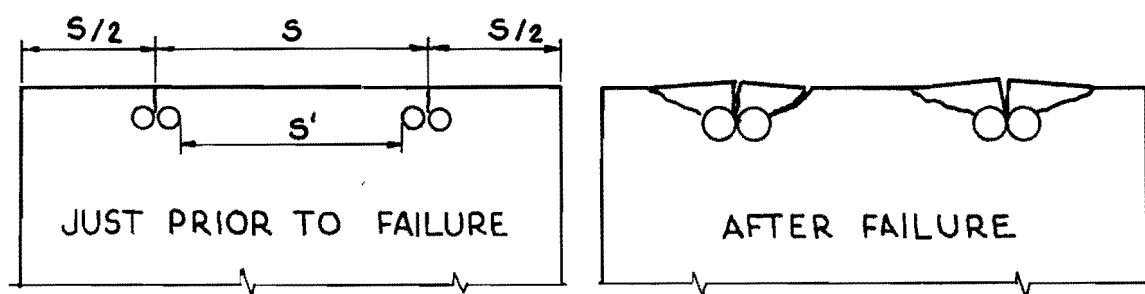
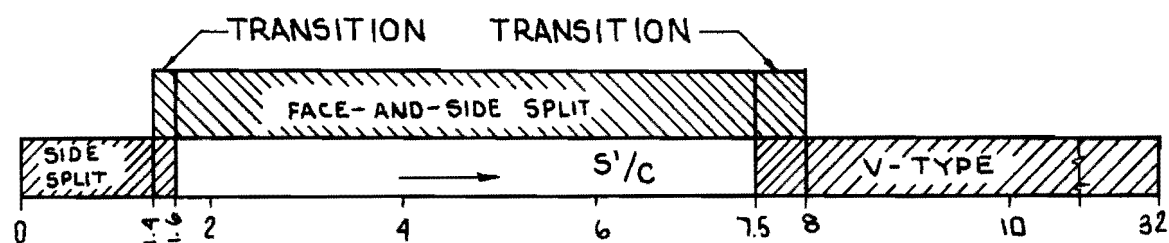
(a) Side split failure mode, $S'/C < 1.4$ (b) Face-and-side split failure mode, $1.6 < S'/C < 7.5$ (c) V-type failure mode, $S'/C > 8.0$ (d) Mode depends on S'/C

Fig. 21. Splitting failure modes.

This imagined average splitting stress at ultimate can now be written as

$$\begin{aligned} \text{Aver. } f_{tu} &= \frac{(a_{s1} f_{s1} + a_{s2} f_{s2})}{\pi D} \cdot D / (S' L_s) \\ &= (a_{s1} f_{s1} + a_{s2} f_{s2}) / (\pi S' L_s) \end{aligned}$$

where L_s is the lap splice lap and a_s is the area of the lapped bars (possibly different) carrying different f_s stresses at the two ends of the splice. If $k = f_{s2}/f_{s1}$ and the two bars are equal in size

$$\text{Aver. } f_{tu} = a_s f_{s1} (1 + k) / (\pi S' L_s)$$

The ideal resistance would be the tensile strength of the concrete which here is arbitrarily taken as $6.4 \sqrt{f'_c}$, a value which seemed to check the split cylinder values reasonably.

If α is now defined as the ratio of computed average f_{tu} to the ideal value of $6.4 \sqrt{f'_c}$,

$$\alpha = \frac{a_s f_{s1} (1 + k)}{6.4 \sqrt{f'_c} \pi S' L_s} = \frac{f_{s1} (1 + k) D^2}{6.4 \sqrt{f'_c} S' L_s} \quad (7)$$

the various test results can be compared, as shown in Fig. 22, with data plotted from Appendix Tables A.1 to A.3. Different bar sizes are coded in this figure and alongside each point is a number representing the splice lap in bar diameters. Also noted alongside is the letter y where the steel yielded, and sometimes also the stress attained.

If one discounts those very low α values in the range of S'/C of 4 to 6 on the basis of their high bar stresses, the dotted line gives a reasonably safe relation between α and S'/C which appears useful as a starting basis for design when f_s is in the range of 60 to 70 ksi and $S'/C \geq 1$. When $C < S'$ the side split failure occurs and C is then not a variable. It is still necessary for the designer to consider ductility,

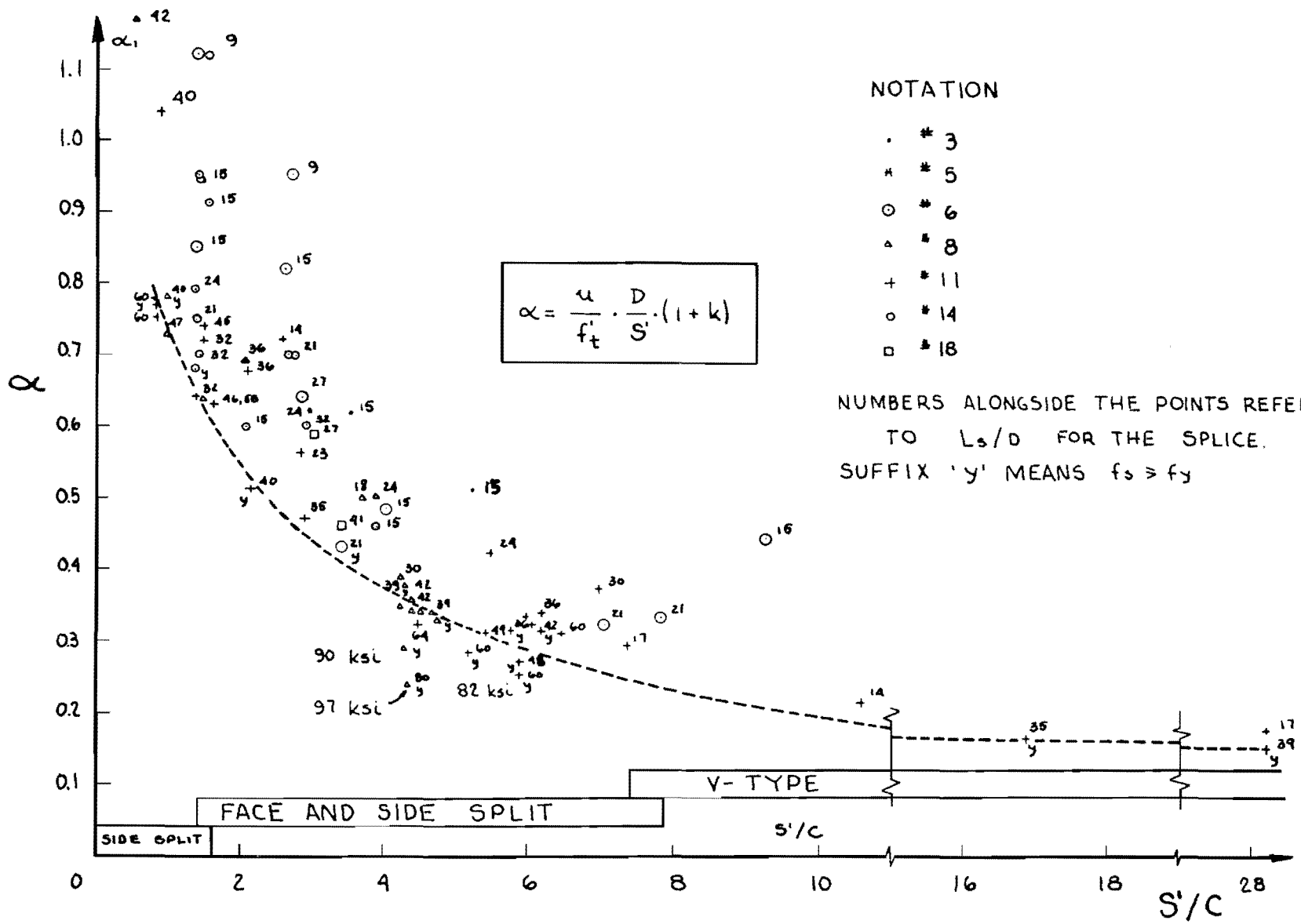


Fig. 22. Variation of α with S'/C . (Same figure as Fig. 2.)

which means designs based on something like $1.25f_y$. This adjustment to design values is covered in Part A where $1/\alpha$ is evaluated algebraically in a form which leads to a relatively simple equation for the required lap length L_s .

Influence of Transverse Reinforcement

Transverse reinforcement around lap splices, whether of stirrups or of spirals, improves splice behavior and increases splice strength. Splitting of concrete over the splices is delayed and slowed. The variation of stress along the splice bars becomes more uniform. A more ductile failure pattern is achieved, although the final collapse (at high strains) may still be sudden. The final failure pattern is still much the same as shown in Figs. 17 and 18.

Strength Contributed by Transverse Reinforcement

The strength evaluation of transverse reinforcement has been shown in Table 6 for all beams of this type tested at The University of Texas at Austin. Explanation of this evaluation is necessary because how steel and concrete cooperate in this case can be discussed more qualitatively than quantitatively.

The primary failure to be resisted is a tension which leads to splitting failure. Since a steel stress of 3000 to 5000 psi represents a tensile cracking strain on the concrete, the two materials can work together efficiently only in an indirect fashion. Nevertheless, Table 6 tabulates f_{st} (col. 7), the added splice bar stress which seems to accrue from the presence of the stirrups or ties. In many cases, especially with the #14 and #18 specimens, it is substantial. It must be surmised that the steel adds to strength (1) by picking up tension where the concrete has split, with a capacity far beyond that of the concrete it replaces and (2) slowing the further spread of splitting and thus helping the concrete indirectly.

The measured strains in the stirrups and spirals led to the stresses plotted in Fig. 23. Although strain gages vary in their readings dependent on their location relative to nearby cracks, the pattern shown indicates resistance is greater near the ends of the splice until failure (P_u)

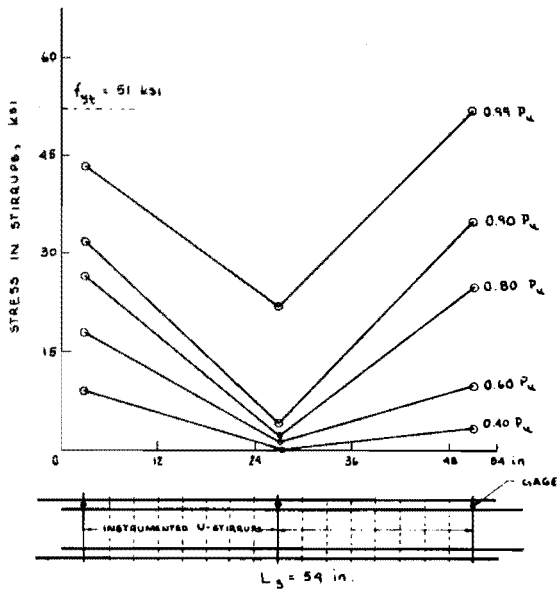
TABLE 6. COMPUTED VALUES OF $1/\alpha_2$ FOR ENCLOSED SPLICES

Investigator	Beam No.	S'/C	α	f_{so} ksi	f_s max. ksi	f_{st} ksi	$\frac{A_v}{A_s} \frac{f_y}{t}$ ksi	$\beta = \frac{1}{\alpha_2}$	Failure Mode
<u>SPIRALS</u>									
Burns*	14S-4	1.04	0.73	39.0	61.0	22.0	40.5	2.94	SS
Krishnaswamy	14S-4	2.88	0.45	23.0	50.0	27.0	41.0	2.38	FS
and	14S-5	2.88	0.45	35.7	69.6	33.9	60.7	-	Flexure
Ferguson	14S-6	2.88	0.45	29.2	60.0	30.8	48.3	2.44	FS
	18S-9	3.04	0.44	33.0	70.4	37.4	66.0	-	Flexure
	18S-10	3.04	0.44	33.8	74.2	40.4	66.0	-	Flexure
	18S-11	3.04	0.44	34.1	62.2	28.1	33.0	1.85	FS
	18S-13	3.04	0.44	27.0	59.4	32.4	52.8	2.57	FS
<u>STIRRUPS</u>									
Ferguson	8F30b	4.35	0.35	44.6	57.0	12.4	19.0	2.44	FS
and	8F36c	4.43	0.34	56.5	61.0	4.5	19.0	6.7	FS
Breen	8F36d	4.26	0.35	64.6	75.5	10.9	31.5	4.46	FS
	8F36e	4.43	0.34	69.5	79.4	9.9	19.0	3.03	FS
	8F36f	4.35	0.35	66.3	79.6	13.3	31.5	3.70	FS
	8F36g	4.26	0.35	59.7	75.3	15.6	19.0	1.92	FS
	8F36h	4.10	0.36	47.1	55.5	8.4	44.5	8.3	FS
	8F36j	4.35	0.35	45.5	63.4	17.9	44.5	3.85	FS
	11R36a	4.56	0.33	59.2	81.7	22.5	39.0	2.71	FS
Briceño and	SP-24	0.90	0.77	36.3	63.7	27.4	12.7	0.83	SS
Ferguson	SP-25	0.97	0.76	26.0	61.6	35.6	21.5	1.07	SS
(Rep. 113-2)	SP-26	1.09	0.73	27.5	59.8	32.3	21.5	1.17	SS
Krishnaswamy	14S-2	2.88	0.45	42.5	59.5	17.0	21.4	1.85	ES
and	14S-3	2.88	0.45	22.5	39.0	16.5	21.4	2.04	FS
Ferguson	14S-7	2.88	0.45	37.4	66.5	29.1	60.7	-	Flexure
	18S-1	3.02	0.44	38.4	65.6	27.2	20.4	1.17	FS
	18S-4	3.03	0.44	37.7	66.0	28.3	50.5	2.87	FS
	18S-5	3.04	0.44	46.0	71.0	25.0	60.6	-	Flexure
<u>HAIRPINS</u>									
Krishnaswamy	18S-2	3.02	0.44	30.6	52.6	22.0	40.8	2.95	FS
and	18S-3	3.02	0.44	49.1	59.5	10.4	14.2	2.13	FS
Ferguson	18S-6S	6.05	0.28	55.7	68.2	12.5	71.3	-	Flexure

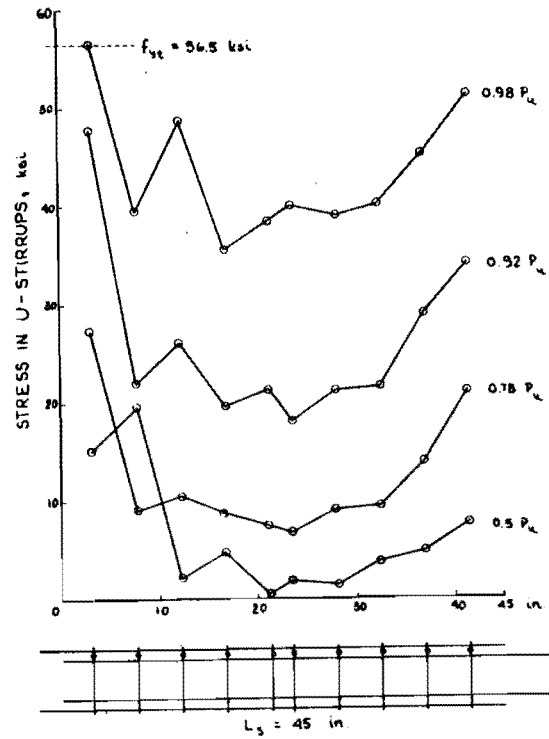
SS = Side Split

FS = Face-and-side Split

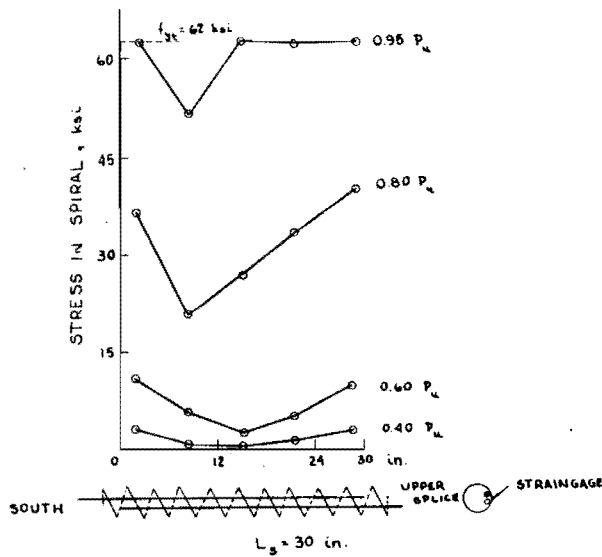
*Burns, Ned H., "The Efficiency of Spiral Reinforcement around Lapped Splices in Reinforced Concrete Beams," MS thesis, The University of Texas, August 1958.



(a)



(b)



(c)

Fig. 23. Stresses in transverse reinforcement (constant moment).

(a) In U-stirrups of 14S-2.

(b) In U-stirrups of 14S-7.

(c) In spiral of 14S-4.

approaches. At failure the transverse steel stress is substantial but it should be noted that a large portion of the steel stress substitutes for a lost concrete splitting resistance rather than adding to it.

In spite of stresses being largely nonadditive, it is expedient to consider the effectiveness of the transverse reinforcement simply in terms of the extra strength it contributes to the splice. In Table 6 α measures the expected efficiency of the concrete and leads to a predicted f_{s0} for the splice without transverse reinforcement. This subtracted from the test f_s (maximum) leaves f_{st} as the addition because of the transverse reinforcement. The equation of splitting resistance then can be written

$$(1 + k)f_s D^2/4 = \alpha 6.4 \sqrt{f'_c} S' L_s + \alpha_2 A_v f_{yt} \quad (8)$$

where the last term represents the added strength from the transverse reinforcement with yield stress f_{yt} based on A_v , the total area of all legs perpendicular to the plane of the splices, and α_2 a constant less than unity. Although α_2 could be calculated directly, it becomes more convenient to use $1/\alpha_2 = \beta$, which is plotted in Fig. 24. There is much scatter as would be expected from this method of differences. Several values run high, which means relatively low efficiencies. Flexural failures were not plotted. Burns used a spiral with very low yield, but three others are unexplained. Most values fall below or near a trend line defining a reasonable

$$\beta = 0.4(1 + 2S'/C) \quad (9)$$

which gives a rough guide as to what can be expected. Spirals gave a little better strength (lower β) but more work needs to be done to define the added strength more closely.

Design Approach for Transverse Reinforcement

Whether data are yet adequate to define design rules closely is debatable, but it should be noted that Eqs. 8 and 9 can be developed into a design procedure which specifies the A_v required to increase the splice steel stress by an amount f_{st} (Table 6).

For design the 1.3 factor used in developing Eq. 3 in Part A to obtain ductility must be introduced into Eq. 8, and is included in Eq. 7 (p. 16 of Part A).

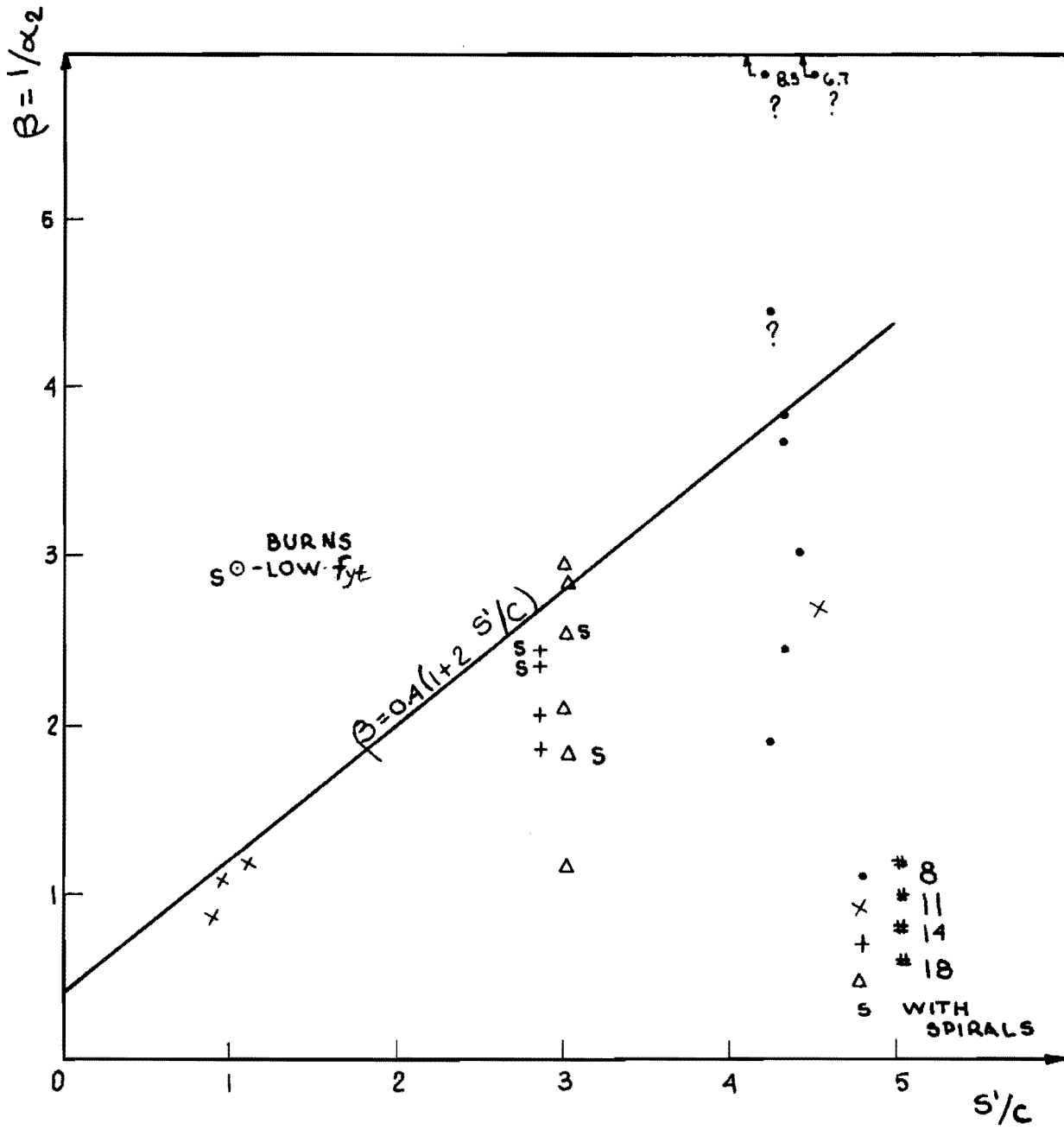


Fig. 24. Variations of β with S'/C .

$$1.3(1+k)f_s D^2/4 = \alpha 6.4 \sqrt{f'_c} S' L_s + \alpha_2 A_v f_{yt}$$

The value of f_s (which is usually f_y) can be somewhat arbitrarily subdivided into f_{sl} to be cared for by L_s and f_{st} to be cared for by A_v , leading to

$$\begin{aligned} 1.3(1+k)f_{st} D^2/4 &= \alpha_2 A_v f_{yt} = A_v f_{yt} / \beta \\ &= A_v f_{yt} / [0.4(1 + 2S'/C)] \end{aligned}$$

$$\begin{aligned} \text{Required } A_v f_{yt} &= 1.3(1+k)f_{st} (D^2/4) 0.4(1 + 2S'/C) \\ &= 0.13(1+k)f_{st} D^2 (1 + 2S'/C) \end{aligned}$$

In a constant moment zone ($k = 1$) this becomes

$$\text{Required } A_v f_{yt} = 0.26 f_{st} D^2 (1 + 2S'/C) \quad (10)$$

The equation can also be solved for the f_{st} provided by a given $A_v f_{yt}$.

Again it should be noted that S'/C is not to be used as less than unity, because then C ceases to act as a variable.

General Design Equations

The basic relationships discussed in this Section B have been modified in Section A into design equations for splice length under various conditions. This portion need not be repeated here.

A P P E N D I X A

N O T A T I O N

A	= area of bar which is spliced, in. ²
A_v	= transverse steel area, counting all legs perpendicular to splice, in. ²
a_{s1}, a_{s2}	= areas of two unequal bars where lapped as a splice, in. ²
b	= beam width, in.
C	= clear cover over splice, in.
D	= bar diameter, in.
f_s	= maximum steel stress at splice, ksi
f_{sl}	= steel stress in splice developed by L_s without help of transverse reinforcement, ksi
f_{so}	= predicted splice strength in absence of ties or spirals, ksi
f_{st}	= increase in steel stress developed by splice because of transverse reinforcement, ksi
f_{su}	= nominal ultimate steel stress = $M_u / (0.9dA_s)$, ksi
f_{s1}, f_{s2}	= defined with k
f'_t	= tensile strength of concrete, psi
f_{tu}	= average computed splitting stress over length of splice, psi
f_y	= yield strength of bar, ksi
f_{yt}	= increase in steel stress developed by splice because of transverse reinforcement, ksi
k	= ratio of smaller stress f_{s2} to larger stress f_{s1} at two ends of a splice
L_s	= splice length, in.
L_{s60}, L_{s40}	= required splice length in 3000 psi concrete to develop 60 ksi or 40 ksi
L_{s60w}, L_{s40w}	= corresponding required splice length for an interior wall splice
M_u	= moment at a splice, i-in.
Σo	= perimeter of bar, in.
P_u	= load-producing failure of splice or beam
S	= center-to-center splice spacing, in.
S'	= clear spacing between splices, in.
t	= overall beam depth, in.
u	= bond stress, psi
α	= ratio of nominal splitting stress to tensile strength of concrete
α_2	= ratio of actual strength added by transverse steel to the nominal strength of such steel
β_2	= $1/\alpha_2$
ϵ_s	= unit strain in steel

A P P E N D I X B

TABLE B.1. α FROM AVAILABLE TEST RESULTS WITHOUT TIES OR STIRRUPS.

Investigator	Beam No.	f'_c psi	b in.	t in.	S in.	C in.	Bar Size	f_y ksi	L_s in.	k	f_s max. ksi	S' in.	$\frac{L_s}{D}$	$\frac{S'}{C}$	α	Failure Mode**
Chinn ^a	D31	4700	3.69	-	3.69	0.83	#3	79.0	5.5	1.00	62.0	2.94	14.6	3.54	0.62	FS
	D36	4410	3.69	-	3.69	0.56	#3	79.0	5.5	1.00	50.2	2.94	14.6	5.25	0.51	FS
K and F	SP-40	3220	7.50	13.13	3.75	0.83	#5	73.0	15.13	1.00	43.1	2.50	24.0	3.00	0.62	FS
Burns	1	3620	6.00	9.00	3.00* (av.)	1.69	#5	66.5	25.0	1.00	67.0	1.75 (av.)	40.0	1.04	0.78	SS
Chinn	D7	4450	3.62	-	3.62	1.27	#6	57.0	11.0	1.00	32.5	2.12	14.6	1.59	0.91	SS
	D9	4380	3.62	-	3.62	1.44	#6	57.0	11.0	1.00	33.5	2.12	14.6	1.47	0.95	SS
	D10	4370	3.62	-	3.62	1.48	#6	57.0	7.0	1.00	25.2	2.12	9.3	1.43	1.12	SS
	D12	4530	3.75	-	3.75	1.62	#6	57.0	16.0	1.00	44.0	2.25	24.0	1.39	0.79	SS
	D13	4820	7.31	-	7.31	1.44	#6	57.0	11.0	1.00	48.8	5.81	14.6	4.05	0.48	FS
	D14	4820	3.69	-	3.69	0.83	#6	57.0	11.0	1.00	31.4	2.19	14.6	2.64	0.82	FS
	D15	4290	7.25	-	7.25	0.62	#6	57.0	11.0	1.00	42.0	5.75	14.6	9.30	0.44	FS
	D17	3580	3.69	-	3.69	0.80	#6	57.0	16.0	1.00	37.9	2.19	21.3	2.74	0.70	FS
	D19	4230	7.31	-	7.31	1.70	#6	57.0	16.0	1.00	59.6	5.81	21.3	3.42	0.43	FS
	D20	4230	3.75	-	3.75	1.42	#6	57.0	7.0	1.00	25.8	2.25	9.3	1.58	1.12	SS
	D22	4480	3.69	-	3.69	0.80	#6	57.0	7.0	1.00	22.9	2.19	9.3	2.74	0.95	FS
	D23	4450	3.62	-	3.62	0.78	#6	57.0	16.0	1.00	37.6	2.12	21.3	2.72	0.70	FS
	D24	4450	7.25	-	7.25	0.81	#6	57.0	16.0	1.00	43.0	5.75	21.3	7.10	0.32	FS
	D25	5100	3.62	-	3.62	1.53	#6	57.0	24.0	1.00	56.1	2.12	32.0	1.38	0.68	SS
	D26	5100	3.69	-	3.69	0.75	#6	57.0	24.0	1.00	53.8	2.19	32.0	2.92	0.60	FS
	D29	7480	3.69	-	3.69	1.39	#6	57.0	11.0	1.00	43.5	2.19	14.6	1.57	0.91	SS
	D30	7480	3.69	-	3.69	1.56	#6	57.0	16.0	1.00	51.5	2.19	21.3	1.40	0.75	SS
	D32	4700	7.25	-	7.25	1.47	#6	57.0	11.0	1.00	46.0	5.75	14.6	3.91	0.46	FS
	D34	3800	3.62	-	3.62	1.49	#6	57.0	12.5	1.00	35.2	2.12	16.6	1.42	0.94	SS
D35	3800	3.62	-	3.62	1.45	#6	57.0	24.0	1.00	52.5	2.12	32.0	1.46	0.75	SS	
D38	3160	4.62	-	4.62	1.52	#6	57.0	11.0	1.00	27.1	3.12	14.6	2.06	0.60	SS	
D39	3160	3.69	-	3.69	1.56	#6	57.0	11.0	1.00	26.2	2.19	14.6	1.40	0.85	SS	
D40	5280	7.38	-	7.38	0.75	#6	57.0	16.0	1.00	50.5	5.88	21.3	7.85	0.33	FS	

TABLE B.2. α FROM AVAILABLE TEST RESULTS WITHOUT TIES OR STIRRUPS

Investigator	Beam No.	f'_c psi	b in.	t in.	S in.	C in.	Bar Size	f_y ksi	L_s in.	k	f_s max. ksi	S' in.	$\frac{L_s}{D}$	$\frac{S'}{C}$	α	Failure Mode**	
Ferguson and Breen	8R18a	3470	17.03	14.97	8.52	1.75	#8	100.0	18.0	1.00	43.4	6.52	18.0	3.72	0.50	FS	
	8R24a	3530	17.12	15.03	8.56	1.67	#8	100.0	24.0	1.00	59.3	6.56	24.0	3.92	0.50	FS	
	8F30a	3030	17.09	14.97	8.55	1.53	#8	75.0	30.0	1.00	52.7	6.55	30.0	4.28	0.39	FS	
	8F36a	4650	17.16	15.00	8.58	1.41	#8	64.0	36.0	1.00	69.5	6.58	36.0	4.66	0.34	FS	
	8F36b	3770	16.94	15.03	8.47	1.40	#8	75.0	36.0	1.00	61.5	6.47	36.0	4.62	0.34	FS	
	8F39a	3650	17.06	15.09	8.53	1.53	#8	64.0	39.0	1.00	74.0	6.53	39.0	4.27	0.38	FS	
	8F42a	2660	17.19	15.09	8.60	1.50	#8	64.0	42.0	1.00	65.7	6.60	42.0	4.40	0.36	FS	
	8F42b	3830	17.16	15.03	8.58	1.45	#8	100.0	42.0	1.00	75.2	6.58	42.0	4.55	0.34	FS	
	8R42a	3310	17.19	15.00	8.60	1.56	#8	100.0	42.0	1.00	71.0	6.60	42.0	4.23	0.35	FS	
	8R48a	3040	17.03	15.00	8.52	1.48	#8	100.0	48.0	1.00	73.0	6.52	48.0	4.40	0.34	FS	
	8R64a	3550	17.09	15.00	8.55	1.52	#8	100.0	64.0	1.00	89.6	6.55	64.0	4.30	0.28	FS	
	8R80a	3740	17.03	15.03	8.52	1.50	#8	100.0	80.0	1.00	97.0	6.52	80.0	4.35	0.24	FS	
	8F36k	3460	9.69	15.09	4.85	1.38	#8	100.0	36.0	1.00	53.1	2.85	36.0	2.10	0.69	FS	
	Briceño and Ferguson	SP-1a	2770	8.00	15.75	4.00	2.00	#8	68.0	47.0	0.75	51.0	2.00	47.0	1.00	0.73	SS
		SP-2a	3920	10.00	13.00	5.00	2.00	#8	68.0	32.0	0.83	57.9	3.00	32.0	1.50	0.69	FS
SP-4a		4350	6.25	20.00	3.13	2.00	#8	68.0	42.0	0.78	54.0	1.10	42.0	0.55	1.17	SS	
Ferguson and Breen	11R24a	3720	24.09	18.09	12.05	1.67	#11	93.0	33.8	1.00	51.5	9.23	24.0	5.5	0.42	FS	
	11R30a	4030	24.09	18.09	12.05	1.31	#11	93.0	42.3	1.00	58.5	9.23	30.0	7.0	0.37	FS	
	11F36a	4570	24.09	18.00	12.05	1.50	#11	73.0	50.6	1.00	64.2	9.23	36.0	6.1	0.32	FS	
	11F36b	3350	24.03	18.00	12.02	1.47	#11	65.0	50.6	1.00	58.9	9.20	36.0	6.2	0.34	FS	
	11F42a	3530	24.00	18.00	12.00	1.48	#11	65.0	59.2	1.00	63.2	9.18	42.0	6.2	0.31	FS	
	11F48a	3140	24.06	18.03	12.03	1.53	#11	73.0	67.7	1.00	73.3	9.21	48.0	6.0	0.33	FS	
	11F48b	3330	24.15	18.22	12.00	1.58	#11	65.0	67.7	1.00	72.0	9.26	48.0	5.8	0.31	FS	
	11R48a	5620	24.16	18.03	12.08	1.50	#11	93.0	67.7	1.00	82.5	9.26	48.0	5.9	0.27	FS	
	11R48b	3100	24.22	18.19	12.11	2.06	#11	93.0	67.7	1.00	71.3	9.29	48.0	4.5	0.32	FS	
	11F60a	2610	23.97	18.09	11.99	1.59	#11	73.0	84.6	1.00	79.3	9.17	60.0	5.8	0.31	FS	
	11F60b	4090	24.00	18.09	12.00	1.50	#11	65.0	84.6	1.00	78.6	9.18	60.0	5.9	0.25	FS	
11R60a	2690	24.00	18.12	12.00	1.41	#11	93.0	84.6	1.00	78.6	9.18	60.0	6.5	0.31	FS		
11R60b	3460	23.97	18.03	11.99	1.75	#11	93.0	84.6	1.00	82.4	9.17	60.0	5.2	0.28	FS		
Chinn	D33	4830	6.80	-	6.80	1.55	#11	-	20.3	1.00	26.0	3.98	14.4	2.58	0.72	FS	

TABLE B.3. α FROM AVAILABLE TEST RESULTS WITHOUT TIES OR STIRRUPS

Investigator	Beam No.	f'_c psi	b in.	t in.	S in.	C in.	Bar Size	f_y ksi	L_s in.	k	f_s max. ksi	S' in.	$\frac{L_s}{D}$	$\frac{S'}{C}$	α	Failure Mode**	
Briceño and Ferguson	SP-1	2800	9.06	24.06	4.53	2.00	#11	65.0	85.0	0.56	48.0	1.71	60.28	0.86	0.75	SS	
	SP-5	3900	9.00	24.13	4.50	2.00	#11	65.0	85.0	0.56	59.0	1.68	60.28	0.84	0.78	SS	
	SP-7	2920	9.31	24.06	4.66	2.00	#11	65.0	57.5	0.70	44.8	1.84	40.78	0.92	1.04	SS	
	SP-12	4250	11.68	20.00	5.84	2.00	#11	65.0	65.0	0.66	71.1	3.02	46.09	1.51	0.72	FS	
	SP-13	3380	14.31	17.00	7.16	2.00	#11	65.0	44.0	0.77	57.5	4.24	31.20	2.12	0.69	FS	
	SP-14	3050	17.00	14.89	8.50	2.00	#11	65.0	33.0	0.83	41.2	5.68	23.40	2.84	0.56	FS	
	SP-15	3340	14.13	17.00	7.07	2.00	#11	65.0	65.0	0.66	64.5	4.25	46.09	2.13	0.51	FS	
	SP-16	3060	14.13	17.06	7.07	3.00	#11	65.0	44.0	0.77	56.3	4.25	31.20	1.41	0.74	SS-FS	
	SP-17	3550	17.06	14.75	8.53	2.00	#11	65.0	50.0	0.74	58.6	5.71	35.46	2.86	0.46	FS	
	SP-21	4190	9.00	24.00	4.50	2.00	#11	65.0	85.0	0.56	59.4	1.68	60.28	0.84	0.76	SS	
	SP-27	3270	15.13	24.13	5.04	2.00	#11	68.0	42.3	0.78	41.0	2.22	30.00	1.11	1.06	SS	
	SP-23	3600	12.00	20.00	6.00	2.00	#11/#9	65.0	65.0	1.03	55.2	3.46	46.09	1.73	0.52	SS	
	Krishna- swamy and Ferguson	SP-32	3280	24.00	12.25	24.00	1.25	#11	67.5	50.0	0.74	72.5	21.18	35.41	16.90	0.16	VS
		SP-33	3360	24.00	11.88	24.00	0.75	#11	67.5	55.0	0.72	75.5	21.18	39.00	28.20	0.15	VS
SP-34		3280	24.00	12.00	24.00	0.75	#11	67.5	36.0	0.81	54.5	21.18	25.50	28.20	0.17	VS	
SP-35		3310	24.00	13.25	24.00	2.00	#11	67.5	20.0	0.90	34.4	21.18	14.19	10.60	0.21	VS	
SP-36		3440	17.50	17.25	17.50	2.00	#11	67.5	24.0	0.88	41.5	14.68	17.00	7.40	0.29	VS	
SP-37		3260	28.00	17.13	7.00 [†]	2.00	#11	67.5	45.0	0.77	69.2	4.18 [†]	31.90	2.12 [†]	0.57	Fig. 15c	
SP-38		2970	11.25	21.38	5.63	2.00	#11	67.5	40.0	0.79	43.5	2.81	28.40	1.41	0.64	SS-FS	
SP-39		3120	21.00	16.88	7.00	2.00	#11	71.7	45.0	0.77	51.1	4.18	31.90	2.12	0.62	FS	
14S-1		2710	20.50	21.00	10.25	2.40	#14	61.0	45.0	1.00	45.6	6.87	26.67	2.86	0.64	FS	
18S-12		3160	27.25	28.00	13.63	3.00	#18	61.3	60.0	1.00	45.2	9.13	26.67	3.04	0.59	FS	
18S-15	2860	27.00	28.10	13.50	2.63	#18	61.3	93.0	1.00	51.5	9.00	41.30	3.42	0.46	FS		

*Actual spacing was 2.38 in. with side cover of 1.19 in.

**SS - Side Split; FS - Face-and-side Split; VS - V-split.

[†]Also 7 in. edge distances; center $S'/C = 2.12$; overall $S'/C = 3.75$.

^aChinn, J., Ferguson, P. M., and Thompson, J. N., "Lapped Splices in Reinforced Concrete Beams," Journal of the American Concrete Institute, Vol. 52, No. 2 (October 1955), pp. 201-213.